An examination of the use of additive manufacturing for small satellite technologies

By

Jacob Nathaniel Easley

Approved by:

Haley Doude (Major Professor)
Keith Koenig
Thomas Anderson
Krystle Dixon (Undergraduate Coordinator)
Jason Keith (Dean, Bagley College of Engineering)

A Thesis
Submitted to the Faculty of
Mississippi State University
in Partial Fulfillment of the Requirements
for the Degree of Bachelor of Science
in Mechanical Engineering
in the Department of Mechanical Engineering

Mississippi State, Mississippi

May 2020

Name: Jacob Nathaniel Easley

Date of Degree: May 1, 2020

Institution: Mississippi State University

Major Field: Mechanical Engineering

Title of Study: An examination of the use of additive manufacturing for small satellite technologies

Major Professor: Haley Doude

Pages in Study: 54

Candidate for Degree of Bachelor of Science

Small satellites and additive manufacturing both have the potential to be disruptive technologies in their respective fields. Small satellites often allow for a more affordable opportunity for small businesses and universities to become involved in space research and science. Additive manufacturing is expanding the opportunity for design and fabrication in a variety of fields including the space industry. Its propensity for customization allows for small satellites to take advantage of these benefits to continue expanding this technology's reach. This study investigates additive manufacturing's potential to do just that.

ACKNOWLEDGEMENTS

There are so many people who are responsible for fostering my success during my undergraduate education. First and foremost, I would like to thank Dr. Haley Doude for her continued support and encouragement throughout my entire undergraduate career and for showing by example what it means to conduct effective and meaningful research. Secondly, I would like to thank Dr. Keith Koenig for helping me expand my horizons on many fronts, especially in the aerospace. Your constant mentorship is greatly appreciated. Thirdly, I'd like to thank Dr. Tommy Anderson for pushing me to expand myself beyond engineering and research and helping me to develop myself into a growing leader as well; the lessons I have learned will follow me throughout my career.

I would also like to thank the whole of the mechanical engineering department for their great support and care of us students. I also thank the Bagley College of Engineering for the incredible resources available to me at any given moment. I also thank the Shackouls Honors College and the Provost Scholars Program for setting me up for success since freshman by urging me to ask the big questions. I am proud to be a part of these three organizations and look forward to continuing to be an ambassador for them.

Last but not least I thank my parents, Darrell and Jennifer Easley, as well as the rest of my family for their constant support of me and my endeavors wherever they may lead.

TABLE OF CONTENTS

ACKNOWLEDGEMENTS ... ii

LIST OF TABLES ... v

LIST OF FIGURES ... vi

CHAPTER

I. INTRODUCTION TO RELEVANT CONCEPTS AND TECHNOLOGIES ... 1

1.1 Small Satellites: Their Novelty and Purpose ... 1
1.2 Introduction to Technical Concepts ... 1
1.2.1 CubeSat Specifications ... 1
1.2.2 Cold Gas Propulsion System ... 4
1.2.3 Additive Manufacturing Overview and Material Selection ... 6
1.3 Abbreviated Literature Review ... 8

II. PRELIMINARY DESIGN AND ANALYSIS OF PROPELLANT TANK AND STRUCTURAL SUPPORTS OF CUBESAT COLD GAS PROPULSION SYSTEM ... 9

2.1 Methodology ... 9
2.1.1 General Design of Propulsion Module ... 9
2.1.1.1 Propellant and Pressurant Calculations ... 10
2.1.1.2 General Design Principles ... 11
2.1.1.3 Pressure Vessel Design ... 13
2.1.1.4 Structural Cube Design ... 15
2.1.1.5 Structural Arm Design ... 19
2.1.1.6 Integration of Components ... 22
2.1.2 Finite Element Analysis ... 23
2.1.3 Testing ... 24
2.1.4 Test Print ... 25
2.2 Results ... 26
2.2.1 Results from FEA ... 26
2.2.1.1 Pressure Vessel Stress Analysis ... 26
2.2.1.2 Propulsion Module Stress Analysis ... 29
2.3 Summary of Preliminary Findings ... 30

III. DESIGN REVISION, PRINTING, AND POST-PROCESSING ... 32

3.1 Design Revisions....32
3.1.1 Model Changes....32
3.1.1.1 Pressure Vessel Port....33
3.1.1.2 Structural Arms....35
3.1.2 Updated Finite Element Analysis....37
3.2 Printing and Post-Processing....43
3.2.1 First Build....44
3.2.2 Finished Build....46
3.2.3 Further Post-Processing....50

IV. FUTURE WORK AND CLOSING REMARKS....51

4.1 Future Work....51
4.2 Conclusion....51

REFERENCES....53

LIST OF TABLES

Table 1.1 Summary of CGP propellants..5

LIST OF FIGURES

Figure 1.1 Schematic of CGP system 4

Figure 2.1 Cross-section of a pressure vessel 15

Figure 2.2 1U geometry requirements as outlined in CubeSat Design Specification.................16

Figure 2.3 Outside structure of CubeSat..17

Figure 2.4 Mass-saving extrusion design..18

Figure 2.5 Mass-optimized CubeSat structure..19

Figure 2.6 One of four structural arms...20

Figure 2.7 (a) Original part, (b) mass-optimized part after topology optimization 21

Figure 2.8 Optimized structural arm 22

Figure 2.9 Final assembly of CubeSat propulsion module 23

Figure 2.10 Test print of CubeSat propulsion module..26

Figure 2.11 Results of FEA for pressure vessel..27

Figure 2.12 Zoomed-in view of port...28

Figure 2.13 Mesh of CubeSat propulsion module 29

Figure 2.14 Stress analysis results of CubeSat propulsion module 30

Figure 3.1 Updated pressure vessel 34

Figure 3.2 Cross-section view of updated pressure vessel 35

Figure 3.3 Updated structural arm 36

Figure 3.4 View of full CubeSat assembly 37

Figure 3.5 Loading and Boundary Conditions on updated model..38

Figure 3.6 Mesh of CubeSat assembly 39
Figure 3.7 Full view of stress analysis visualization 40
Figure 3.8 Cross-section view of stress analysis visualization 41
Figure 3.9 Vertical cross-section view including maximum stress point 42
Figure 3.10 Horizontal cross-section view 43
Figure 3.11 Example of bowing defect in the CubeSat 44
Figure 3.12 Example of knife edge defect in the pressure vessel section....................45
Figure 3.13 Frontal view of completed CubeSat build 46
Figure 3.14 Top view of completed CubeSat build 47
Figure 3.15 Frontal diagonal view of completed CubeSat build 48
Figure 3.16 Minor absence of adhesion on upper pressure vessel....................49
Figure 3.17 Slight abrasion on CubeSat 50

CHAPTER I

INTRODUCTION TO RELEVANT CONCEPTS AND TECHNOLOGIES[1]

1.1 Small Satellites: Their Novelty and Purpose

The aerospace industry in the USA and the world are at a period of much growth in all sectors. One of the most notable areas of rapid growth the small satellite industry. Small satellites have the unique quality of having the ability to perform scientific missions in space at a fraction of the cost and time of traditional satellites, thus opening up an entire industry that can be reached by not only large aerospace firms and defense contractors but also small businesses and universities. In order to ensure the efficiency and efficacy of small satellite systems, certain requirements have been made for a class of small satellites called “CubeSats.”

1.2 Introduction to Technical Concepts

A number of technical requirements exist for CubeSats that ensure a standardized system of design so that these systems can be effectively incorporated into current spacecraft and launch vehicles.

1.2.1 CubeSat Specifications

CubeSats have certain dimensional standards to allow for efficient design and integration of CubeSat systems from a diverse range of universities and institutions. California Polytechnic

[1] This chapter is a slightly modified version of “Additive Manufacturing of Propellant Tank and Structural Supports of CubeSat Cold Gas Propulsion System” published in AIAA Propulsion and Energy Forum 2019 conference proceedings and has been reproduced here with the permission of the copyright holder.

State University, who along with Stanford University developed these CubeSat specifications, wrote in CubeSat Design Specification that a CubeSat is categorized by its size, often denoted in multiples of "1U" where a 1U CubeSat denotes a cubic satellite with side lengths of ten centimeters [1]. Further CubeSat identifiers include 2U, 3U, and 6U CubeSats (along with several other combinations) which simply denote multiple 1U-sized cube stacked on each other or placed beside one another. Further fundamental design specifications laid out in the CubeSat Design Specification include the following [1]:

> **3.1.4** Any propulsion systems shall be designed, integrated, and tested in accordance with AFSPCMAN 91-710 Volume 3.
>
> **3.2.10** The maximum mass of a 1U CubeSat shall be 1.33 kg.
>
> **3.2.14** The CubeSat center of gravity shall be located within 2 cm from its geometric center in the X and Y direction.
>
> > ***3.2.14.1*** The 1U CubeSat center of gravity shall be located within 2 cm from its geometric center in the Z direction.

Although several more design specifications are required when designing and constructing a full CubeSat configuration, this study will focus on the four specifications above as they most apply to the design of the CubeSat's propulsion system. To further expound on certain restrictions, some relevant specifications from the AFSPCMAN 91-710 Volume 3 are listed below [2]:

12.1.5.3.1.1. A detailed and comprehensive stress analysis of each pressure vessel and pressurized structure shall be conducted under the assumption of no crack-like flaws in the structure**.**

12.1.7.1. All pressure vessels and pressurized structures shall possess sufficient strength to withstand limit loads and maximum expected operating pressure (MEOP) in the expected operating environments throughout their respective service lives without experiencing detrimental deformation.

12.1.7.2. All pressure vessels and pressurized structures shall also withstand ultimate loads and design burst pressure in the expected operating environments without experiencing rupture or collapse.

12.1.16.1. Metallic materials shall be selected on the basis of proven environmental compatibility, material strengths, fracture properties, fatigue-life, and crack growth characteristics consistent with the overall program requirements.

12.2.2.7.1. Acceptance tests shall be conducted on every pressure system element before commitment to flight. Accept/reject criteria shall be formulated before tests.

Similar to the CubeSat Design Specification document, the document cited above includes many more restriction statements, but only those most relevant to the study are listed.

1.2.2 Cold Gas Propulsion System

Cold gas propulsion (CGP) is one of the simplest propulsion systems utilized by CubeSats. A CGP system consists of a pressure tank, valves, and cold gas thrusters [3]. Thrust is generated simply by dispelling a gaseous fluid through the thrusters into its surroundings. Multiple thrusters can be configured and pointed along different axes to allow for attitude control. The greatest advantage of utilizing a CGP system is its simplicity. The propellant is not heated nor are any electronic components needed besides those to open the valves. One disadvantage of CGP, though, is the proportionality of the pressure tank pressure to thrust [4]. As the mission time increases and propellant is depleted, the generated thrust decreases. CGP also has a much lower specific impulse (Isp) compared to other propulsion technologies such as liquid or electric propulsion, but integrating complex liquid and electric propulsion systems greatly increases the cost of production and testing. This makes CGP a reasonable choice for simple 1U or 2U CubeSat 3 systems designed by universities or small companies who do not require complex propulsion systems or very large fuel efficiencies. A diagram of a CGP system is shown in Fig. 1.1.

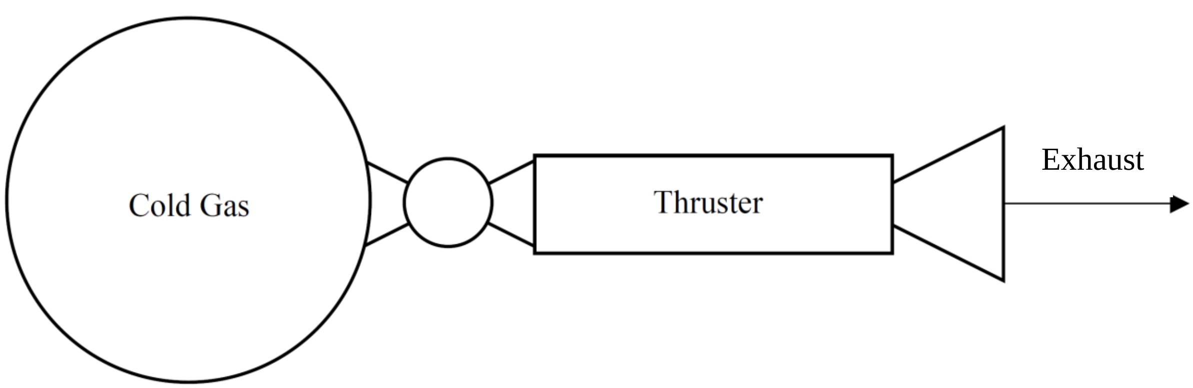

Figure 1.1 Schematic of CGP system

Many propellants have been studied for use in CGP systems, some which are summarized in Table 1.1 below provided by Anis [3]:

Table 1.1 Summary of CGP propellants

Propellant	Molecular Weight (Kg/Kmole)	Density (g/cm^3)	Specific Thrust (s)	
			Theoretical	Measured
Hydrogen	2.0	0.02	296	272
Helium	4.0	0.04	179	165
Nitrogen	28.0	0.28	80	73
Ammonia	17.0	Liquid	105	96
Carbon dioxide	44.0	Liquid	67	61

Liquid propellants such as ammonia and carbon dioxide have the advantage of being more dense than gaseous propellants, thus leading to a greater amount of propellant able to be stored. However, liquid propellants are not ideal in a simple CubeSat configuration as they would require a method of pressurizing the propellant tanks to minimize sloshing effects. Hydrogen and helium provide a greater specific impulse than nitrogen, but their low molecular weights require a larger tank which leads to greater mass and greater costs [3]. Therefore, nitrogen gas is the ideal propellant for this study.

Another key factor in choosing a CGP system is the viability of using additive manufacturing to construct the pressure vessel and structural components. Large amounts of flexibility are gained by incorporating additive manufacturing, but certain limitations must be kept in mind, which will be detailed in Section II.C. Simplicity is the key to promoting the widespread use and viability of additive manufacturing. Therefore, its implementation must begin with simple systems. After the viability of additive manufacturing is confirmed with simple systems, it can be further implemented with more complex configurations. This principle is what makes a CGP system a viable option for additive manufacturing. Once additive manufacturing proves to be a reliable and efficient method of manufacturing CGP systems, it can be adapted for more complex systems.

1.2.3 Additive Manufacturing Overview and Material Selection

Additive manufacturing (AM) is known as a flexible and precise manufacturing process. Its name comes from its process of adding material layer by layer onto a build plate or substrate in order to build a component from the bottom up. It often uses metal powder as its building material and a laser to fuse the powder to the previous layer. This process is in direct contrast to traditional subtractive manufacturing in which material is cut away from an initial block of material. AM has the stark advantage of allowing the building of more complex geometries of which traditional milling tools would have a difficult time shaping. AM is becoming very prevalent in the aerospace industry where rapid prototyping is required.

The particular AM machine used in this study is a Renishaw AM 400. This machine utilizes a type of AM called selective laser melting (SLM) or powder bed fusion (PBF). The defining aspect of this technology is that a blanket of powder is swept over the entire substrate to begin the build. The laser then selects where to melt the powder based on G-code provided by the computer. After the first layer is finished, more powder is spread over the entire substrate area and the process repeats until all layers are built.

Additive manufacturing has a number of limitations to consider when building a part. A critical limitation is the overhang angle of a build, which is the effective angle from one layer to the next. If the angle is too large from the vertical axis to edge of layers, each subsequent layer will not have enough material on which to be founded. Even if this material is melted, the residual stresses caused from overhanging often deform the material to an unusable geometry. This overhang issue can be partially resolved by incorporating skeletal support structures built from the substrate to the designed part. These structural components must be machined off once the build is finished so it is important to take into account how easily support structures can be removed, especially for internal geometries. Another limitation to consider is the dimensional limitations of powder bed fusion. Specifically, the dimensions of the Renishaw AM 400 are 248 mm by 248 mm by 285 mm. These dimensions need to be considered when designing the pressure vessel for the CubeSat cold gas system.

The Renishaw AM 400 supports a wide range of materials from titanium alloys to steels to aluminum alloys. Preliminary designs incorporated an aluminum-silicon alloy AlSi10Mg because of aluminum alloys' high strength-to-weight ratio, response to strengthening mechanisms, and lack of ductile to brittle transition [5]. The latter property is especially beneficial for a cold gas system in which the propellant will remain at relatively low temperatures compared to propulsion systems incorporating combustion. Additionally, the silicon increases creep and corrosion resistance while magnesium induces hardening through precipitations [6]. AlSi10Mg has had ample success as a material used in additive manufacturing and is relatively inexpensive and easily accessible compared to other alloys. Another potential material was a titanium alloy, Ti-6Al-4V. Ti-6Al-4V (Ti64) is known for its very high specific strength but also has the disadvantage of being more expensive [5]. Ti64 is also characterized by its high yield strength, high tensile strength, and low ductility [7]. The fatigue behavior of Ti64 is also similar to its standard wrought counterpart [8]. Though AlSi10Mg has very much potential to be a good material for the CubeSat, Ti64 was chosen for this study because of its much higher yield strength of 985 MPa compared to AlSi10Mg's 206 MPa [9,10].

1.3 Abbreviated Literature Review

Several studies have been conducted researching the potential use of additive manufacturing in propulsion systems. On a macro-scale, Marshall Space Flight Center has had ample success additively manufacturing a copper combustion chamber [11]. The research being done at Marshall is proving AM's viability as a manufacturing process to create components to withstand high pressures and temperatures. More relevant to CubeSat systems are a few studies that have implemented AM in their designs. Another group at Marshall used AM to print several components of a 6U CubeSat including the propellant tanks, which withstood pressures of up to 2000 psi [12]. A group from the University of Southampton and Surrey Satellite Technology Ltd incorporated AM in their design of a heat exchanger for a resistojet propulsion system for satellite technologies [13]. ATK Space Systems, Inc., has also had success in the additive manufacturing of a pressure vessel shell [14]. Aerojet Rocketdyne has had ample success with printed titanium components for some of their thrusters and propulsion systems [15]. Two more studies constructed cold gas propulsion systems for AM [16,17]. A more extensive overview of AM as it pertains to small satellites was written by Gaudenzi et al. [18]. This is not meant to be an exhaustive list of literature containing all instances of this technology; rather, this brief overview is meant to introduce the idea that AM for propulsion systems is already being done and has had good success in the past as well as introduce others who have devoted time to increasing the development of this technology.

CHAPTER II

PRELIMINARY DESIGN AND ANALYSIS OF PROPELLANT TANK AND STRUCTURAL SUPPORTS OF CUBESAT COLD GAS PROPULSION SYSTEM[2]

This study follows much of the entire design process from initial design to simulation to future testing. Examples from past studies were in some cases used as benchmarks for certain aspects of the project.

2.1 Methodology

Two studies in particular are most similar to the current in terms of size and manufacturing methods [16,17]. In one study, a number of imperfections were found across the build due to its rigid shape and internal baffles. In the second study, the presence of a large electron beam weld increases complexity; it was seen in this study as well that the tank ruptured at the seam of this weld. Both of the studies' limitations can be eliminated simply by applying the technique used to design the propellant tank of this study.

2.1.1 General Design of Propulsion Module

The design of the propulsion module involved not only calculations for the pressure vessel but also adherence to proper additive manufacturing design techniques as well as simulation of the system to ensure viability.

[2] This chapter is a slightly modified version of "Additive Manufacturing of Propellant Tank and Structural Supports of CubeSat Cold Gas Propulsion System" published in AIAA Propulsion and Energy Forum 2019 conference proceedings and has been reproduced here with the permission of the copyright holder.

2.1.1.1 Propellant and Pressurant Calculations

To properly evaluate the geometrical dimensions of the pressure vessel as well as the pressure inside the vessel, some preliminary calculations need to be made. This begins by evaluating the necessary initial propellant mass using the relationship between total ΔV, specific impulse, standard gravity, wet mass, and dry mass as detailed in Tsiolkovsky's rocket equation. The term "wet mass" refers to the mass of the spacecraft while full of propellant; "dry mass" refers to the mass of the spacecraft after all propellant has been expelled. Tsiolkovsky's rocket equation is shown below in equation 2.1:

$$\Delta V = I_{sp} g_0 \ln \left[\frac{m_0}{m_f}\right] \tag{2.1}$$

Initially, values for vessel volume and dry mass had to be estimated to gain the ability to design the vessel. Once the vessel was designed and modeled, more accurate values were inputted into the functions to calculated final values for pressure and geometrical requirements. The ΔV value of 15 m/s was determined through investigation of other small satellites for orbital maneuvers and attitude adjustments. Using these parameters, the wet mass of the spacecraft was found from which the dry mass was subtracted to find the total propellant mass.

The necessary pressure of the system was calculated using ideal gas relationships and properties of nitrogen gas. Additionally, the operational temperature of the spacecraft was needed to find this pressure. This temperature estimate is not a trivial one because of the path a CubeSat takes while orbiting the Earth. Namely, the spacecraft experiences sunlight and darkness many times through a typical day's time. The limiting case in this study was confined to when the spacecraft will reach peak temperatures because of the increase in pressure that corresponds to this increase in temperature. This temperature is estimated to be around 280 Kelvin. It is true that continual cyclic thermal states of the spacecraft could induce thermal fatigue on the spacecraft, but the range of temperatures the spacecraft will experience is relatively low, so the risk of thermal fatigue effects is unlikely especially given titanium's fatigue behavior.

Using these parameters, the necessary pressure in the CubeSat to perform its mission is 1100 psi. This includes the small changes that arise from evaluating more accurate dry mass and volume values.

2.1.1.2 General Design Principles

As mentioned, the primary goal of this study is to design the pressure vessel of the CGP system while adhering to the principle of designing for additive manufacturing. Namely, design considerations need to be accounted for in the areas of enclosed voids, surface finish, and strength and flexibility [19]. Because of the basic manufacturing processes of an SLM or powder bed system, in which subsequent layers of powder are laid down, enclosed voids will trap powder inside the part. The powder must flow out through some sort of opening or hole. This is an especially important consideration given that a pressure vessel is essentially an enclosed void. Therefore, the design used in this study incorporates a small opening through which the powder can be released and that can also be used for valve installation. Secondly, surface finish is an important issue to consider especially when designing a component that will house a fluid. It is important to have the inside of the pressure vessel as smooth as possible to eliminate any viscous effects, although these effects will already be minimized because the fluid remains stagnant for most of its lifetime. This can be solved relatively easily through post-processing procedures such as rumbling, bead blasting, or sanding [19]. Thirdly, it is important in this study to consider the non-equiaxed microstructure and mechanical properties of components that are built up layer by layer. However, this characteristic of powder bed systems can be advantageously incorporated into the pressure vessel design. Using a finite element model (FEM), the area of greatest stress and strain can be found. From this information, it is possible to construct the part such that the anisotropic properties of the finished print align with the areas of greatest stress and strain in the design. This allows for efficient use of material and ensures that structural integrity is achieved.

Further considerations must be made to ensure successful additive builds, which largely focus on the addition of support material [20]. The flexibility of AM comes at certain costs regarding some build geometries and orientations, but these costs can be mitigated if one focuses on new design principles. Most importantly, this study aims to design the pressure vessel in such a way as to minimize any overhangs and rigid geometries. Solorzano mentions in his dissertation that the largest issue to their design is that it pushed the capabilities of AM [21]. The design was much too blocky with rigid edges and turns, which required the addition of internal baffles to support the build. Even the internal baffles had rigidity to them. The issue was that this group designed the vessel, and then later modified it for AM. Contrarily, this study aims to build from the ground up on the ideas of AM by minimizing these problematic structures. Building a simple shape such as a cylinder allows for a vertical build orientation and ensures identical axial properties for the vessel. Furthermore, this cylindrical design avoids sharp turns by incorporating rounded heads on the ends of the cylinder. These rounded heads avoid the overhang limits of AM, which allows for a simple build not requiring a welding of two parts.

Another way this study aims to adhere to the design principles of AM is to take advantage of the net-shaping capabilities of fusion-based AM. Specifically, this study focuses on building the propulsive and structural components as one part, which is nearly impossible with subtractive manufacturing. More than anything, building the propellant tank and structural systems as one uses the flexibility of AM as a way to increase the simplicity and reliability of the part’s design. The structural components not only support the CubeSat and its payloads but also act as support for the pressure vessel itself, minimizing the stresses and strains on the vessel and ensuring its structural integrity and shape. This CubeSat will consist of a pressure vessel, a cube-like structure, and support arms to connect the vessel and cube. These supports arms will be evaluated in terms of their effectiveness in minimizing material while containing the stresses. Then, a simplified topology optimization can be performed to minimize material used. This optimization is kept to a minimum, however, since oftentimes topology optimizations cause parts to have such complex geometries that they become difficult for AM machines to build [21].

2.1.1.3 Pressure Vessel Design

Finding the necessary pressure in the pressure vessels allows for the design of the CubeSat to come to fruition. Specifically, the thickness of the pressure vessel is found through two equations for sizing cylindrical pressure vessels as found in the pressure and boiler code ASME [22].

The pressure at which these thicknesses are evaluated is higher than the calculated maximum operating pressure of the system to account for safety factors. CubeSat Design Specification requires a safety factor of 1.5 while ASME Pressure Vessel and Boiler Code requires a much higher safety factor. In this case, the ASME code does not need to be followed because the vessel is smaller the diameter at which ASME code is required. Because of this, a safety factor of 1.5 is sufficient for design. However, one of the issues that arises with additive manufacturing is ensuring an absence of porosity in the walls of the pressure vessel. To ensure that porosity is not an issue, the thicknesses of the vessel are scaled upward so that the minimum thickness of the vessel is no less than 1 mm. Equation 2.2 is used to evaluate the thickness of the cylindrical portion of the pressure vessel given multiple parameters in equation 2.2.

$$t_c = \frac{P_{max} \cdot R}{S \cdot E - 0.6 \cdot P_{max}} \tag{2.2}$$

The relevant parameters are as follows: *tc* is the thickness of the cylindrical portion of the pressure vessel, *Pmax* is the maximum pressure the vessel will experience, *R* is the radius of the pressure vessel, *S* is the maximum allowable stress in the vessel, and *E* is the weld joint efficiency of the CubeSat.

The second equation used for sizing the vessel is given by equation 2.3 for elliptical head shapes, which assume that half of the mid-axis equals one-fourth of the inside diameter of the head skirt [22].

$$t_h = \frac{P_{max} \cdot R}{2 \cdot S \cdot E - 0.2 \cdot P_{max}} \tag{2.3}$$

The relevant parameters are as follows: *th* is the thickness of the cylindrical portion of the pressure vessel, *Pmax* is once again the maximum pressure the vessel will experience, *R* is once again the radius of the pressure vessel, *S* is once again the maximum allowable stress in the vessel, and *E* is once again the weld joint efficiency of the CubeSat. Figure 2.1 illustrates a cross-section of the vessel.

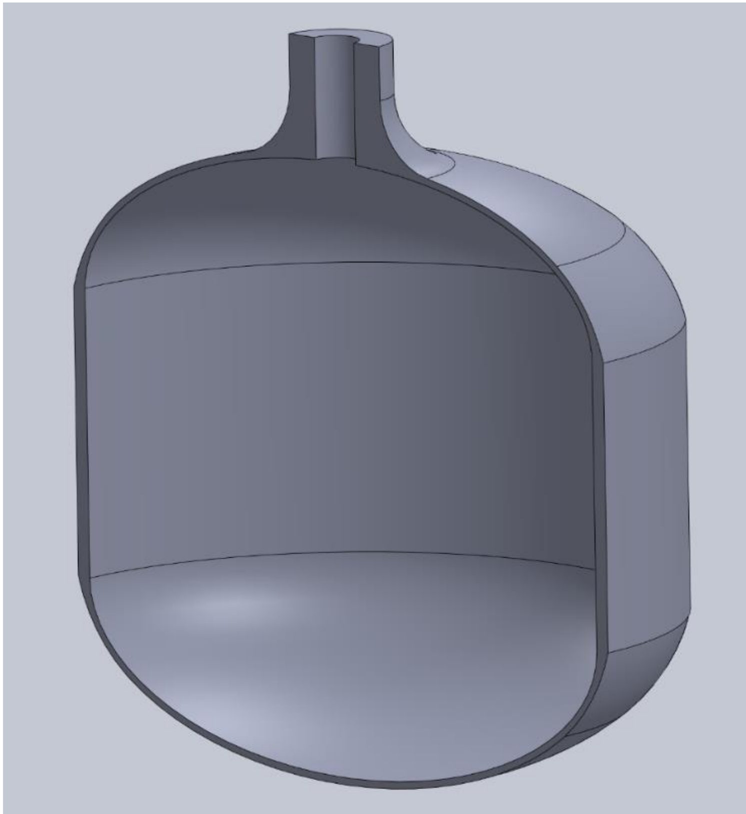

Figure 2.1 Cross-section of a pressure vessel

Using these equations yields a t_c of 1.235 mm and a t_h of 0.609 mm. To ensure an absence of porosity in the part, the cylindrical shell thickness and head thickness have been scaled upward to 2 mm and 1 mm, respectively as seen in Fig. 2.1 above.

It should also be noted that a base and then extrusion are added to the top of the vessel to act as a drain hole as well as a port for a valve to aid in hydrostatic tests.

2.1.1.4 Structural Cube Design

The structural or cube-like portion of the CubeSat was design simply using the geometric standards outlined in CubeSat Design Specification [1]. An image from this document is shown in Fig. 2.2 below.

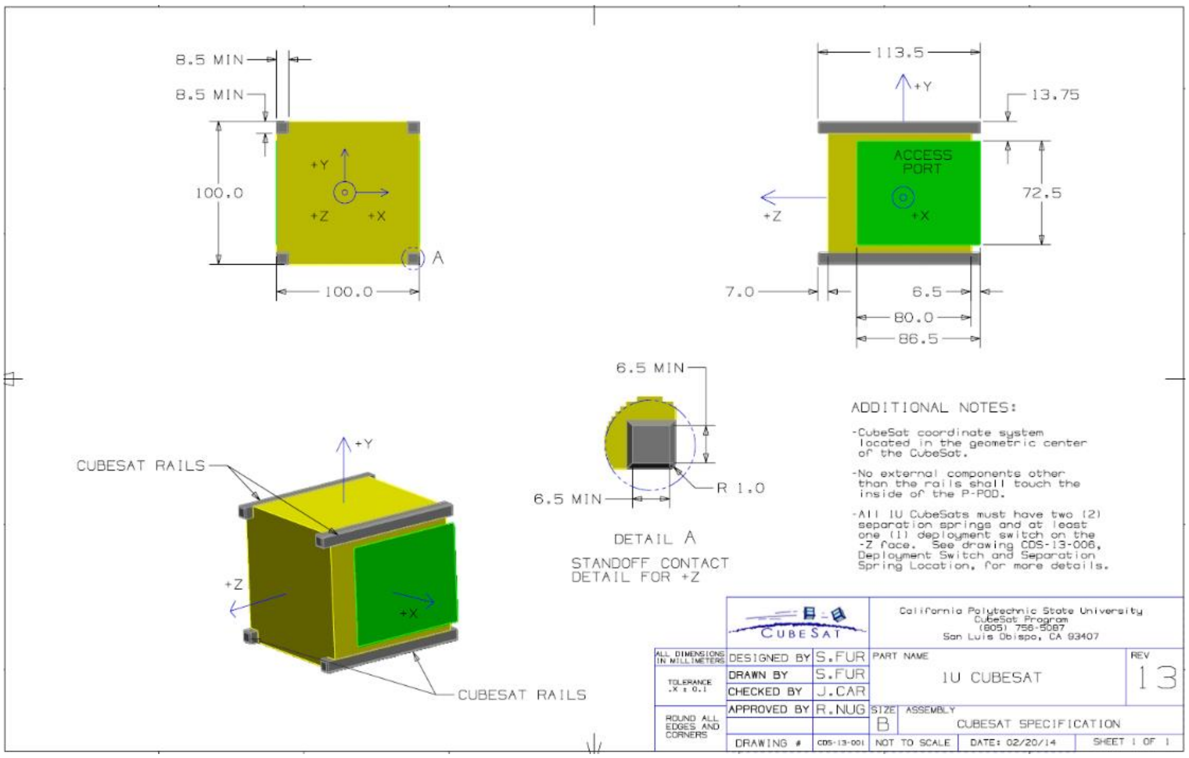

Figure 2.2 1U geometry requirements as outlined in CubeSat Design Specification

Adhering to these specifications make it relatively simple to model the outside structure of the CubeSat as seen in Fig. 2.3 below.

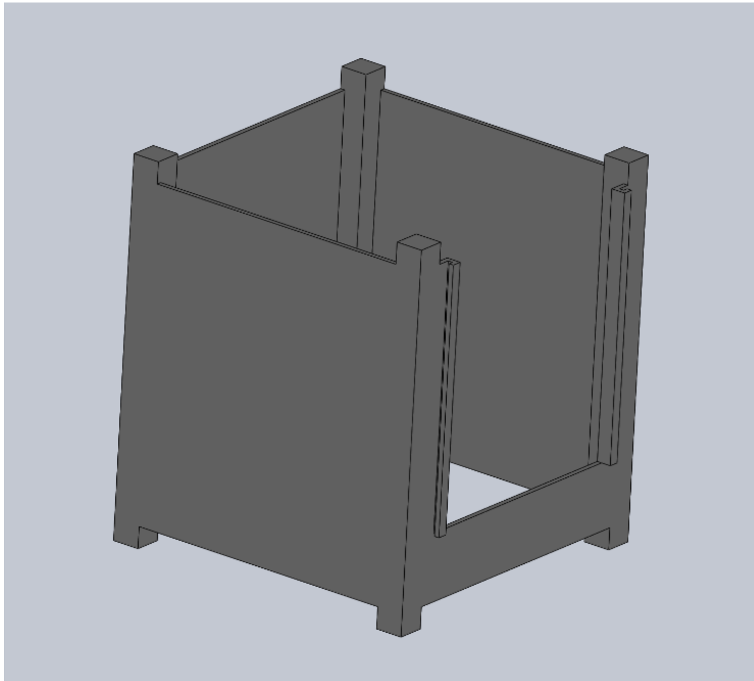

Figure 2.3 Outside structure of CubeSat

However, one improvement that can be made to the design in Fig. 2.3 is eliminating mass from the side walls of the structure. These walls are more for geometric and sizing requirements than for actual structural integrity, so much of the mass can be taken out. Great care needs to be taken however to ensure that the part is printable using AM. Specifically, any extrusion taken from the walls must adhere to the general principles of overhanging structures for metal AM. This means that overhang angles should be restricted to less than 45 degrees. One mass-saving design is shown in Fig. 2.4.

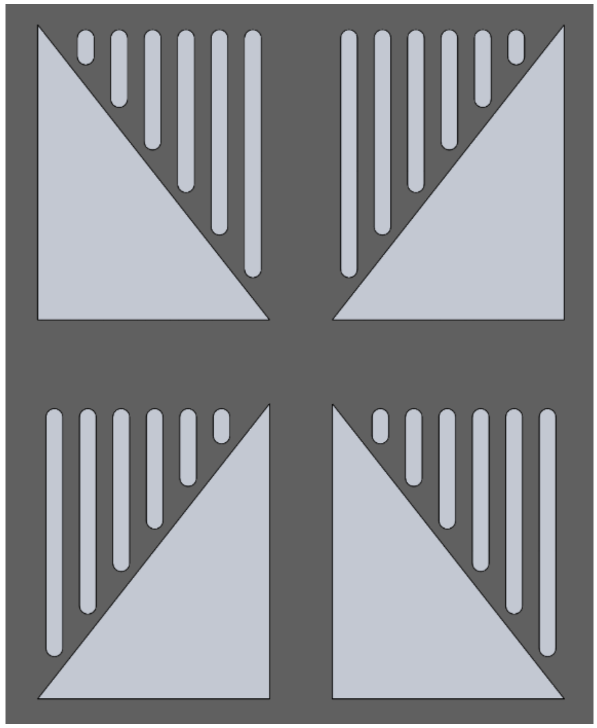

Figure 2.4 Mass-saving extrusion design

Incorporating this design on all three walls yields a 16% mass savings in the structural portion of the CubeSat. A final model of the structure is shown in Fig. 2.5.

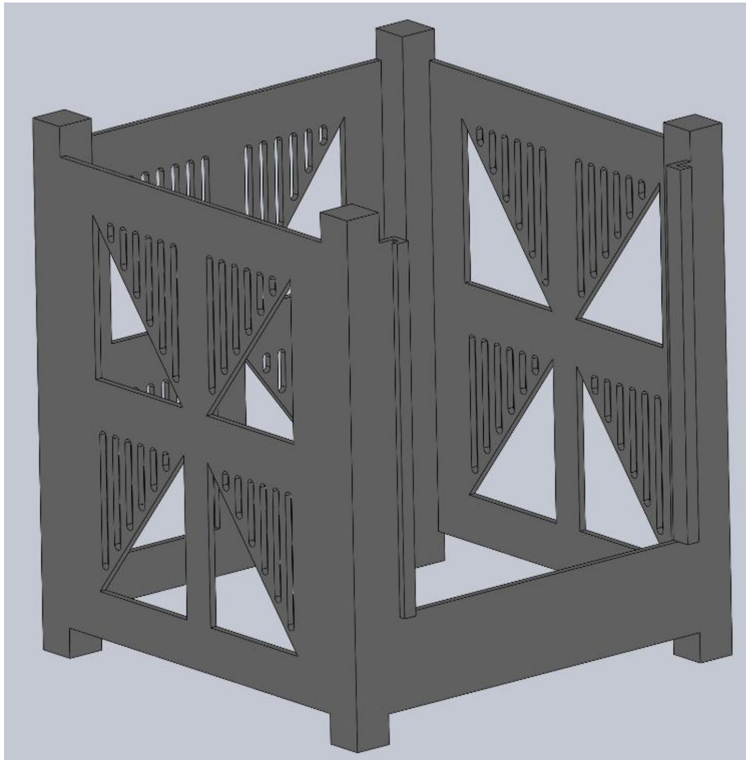

Figure 2.5 Mass-optimized CubeSat structure

2.1.1.5 Structural Arm Design

The last element necessary for the design of the CubeSat propulsion module is the component that connects the outside cube structure to the pressure vessel. These structural arms also act as extra support for the pressure vessel. A topology optimization (TO) was used to design these arms to be mass efficient. This TO was run in Abaqus, the same software used in the stress analysis portion of this study. To perform this TO, a beginning structure was modeled connecting the pressure vessel to each corner of the structure. A model of this component is shown below in Fig. 2.6.

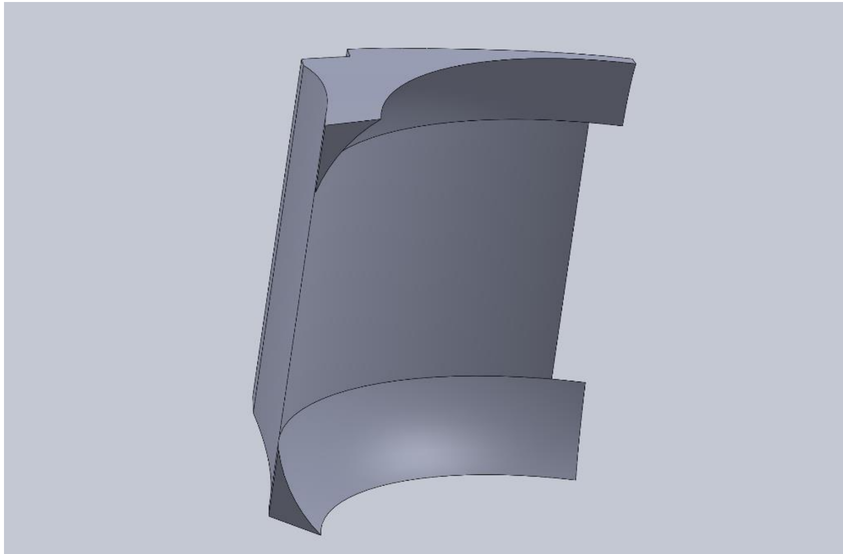

Figure 2.6 One of four structural arms

To perform the TO, first a stress analysis had to be performed on the part which required creating an element mesh for the part and inducing load and boundary conditions. Then the TO was set up in Abaqus by defining an objective function and a constraint. The objective function was to minimize the strain energy of the part, and the constraint was to limit the volume to a small fraction of the original volume. The optimization was then run for 25 cycles to determine the most mass-optimized component to act as a structural arm. The mesh of the original part is shown in Fig. 2.7a, and the output of the TO is shown in Fig. 2.7b.

Figure 2.7 (a) Original part, (b) mass-optimized part after topology optimization

The design of the optimized part is then built fully dense to fix the issue of void areas. It should be noted that the TO is not the main objective of this study. Rather, the TO was performed in an effort to provide a preliminary, mass-efficient design for the structural arms. Thus, a more sophisticated and in-depth study could certainly be performed on the TO portion of this research. Nevertheless, the fully modeled structural arm incorporating design from the TO is shown below in Fig. 2.8.

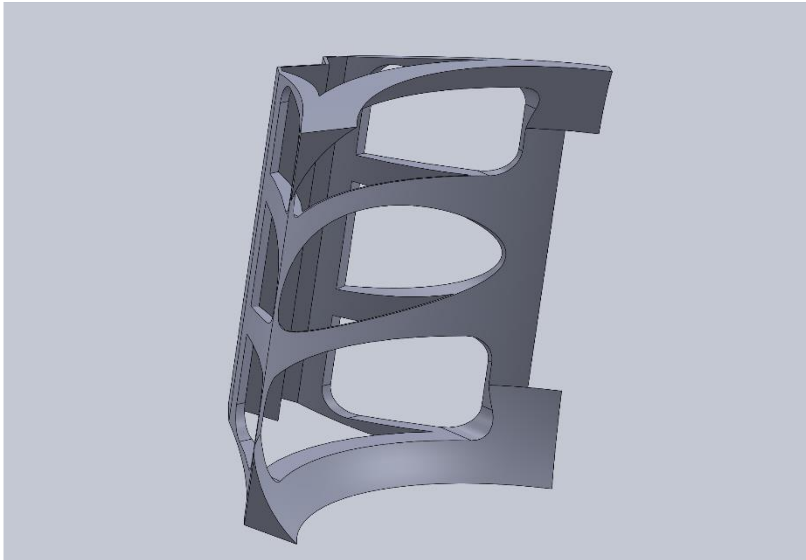

Figure 2.8 Optimized structural arm

2.1.1.6 Integration of Components

After each portion was individually modeled, the components were integrated into an assembly in SolidWorks through a series of mates. This final assembly is seen in Fig. 2.9.

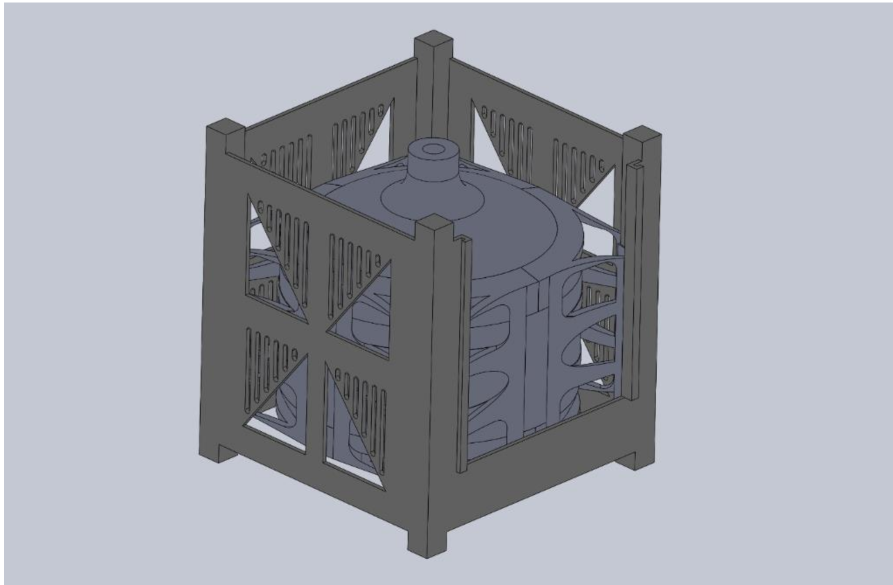

Figure 2.9 Final assembly of CubeSat propulsion module

2.1.2 Finite Element Analysis

The basic principle behind finite element analysis (FEA) is the idea of designing by analysis rather than by formulas [23]. Formulas are good tools for gaining preliminary measurements and design requirements, but ultimately the variability in pressure vessel design makes an individual analysis of each pressure vessel a more accurate judge for stress analysis. Additionally, an FEA can be performed linearly or nonlinearly. A nonlinear FEA assumes that pressure directions change as an object deforms; thus, the change needs to be considered as the vessel deforms. Linear analysis, on the other hand, assumes that the change in geometry is negligible and that the direction of pressure can be assumed the same [24]. Performing a nonlinear analysis will allow conclusions to be made about the realistic amounts of deformation that could occur. If little to no deformation occurs, a linear analysis may be suitable for the design.

Normally, axisymmetric elements can be chosen for pressure vessels to simplify analysis and reduce runtimes. However, this approach was not reasonable for this study's pressure vessel because of the integration of structural support that is not axisymmetric. Instead, 3D tetrahedral or brick elements will be used to model the geometry of the pressure vessel and the support structures. Using brick elements will increase runtime but will also provide more accurate results. However, the complex geometry of the part yields a necessity for tetrahedral elements, which are used throughout the study.

Initial runs incorporated the most refined meshing at the points of contact between the tank and the structural components with the goal of reaching mesh convergence at these points and the tank surface to ensure accurate measurements for stress concentrations. Boundary conditions must also be considered for the stress analysis. In this case, the primary boundary condition is the hole of the pressure vessel because this is where a fitting will be installed for hydrostatic testing.

The goal of performing the FEA is to gain reasonable estimates into stress concentrations of the additively manufactured tank and structural supports. This was done in this study by simplifying the case to an isolated pressure vessel without structural supports made out of a similar material using traditional manufacturing methods. This hypothetical case was used to make estimates of the maximum pressures that the vessel could withstand. Then, the FEA's purpose was to confirm those initial estimates, and support structures were added. Ultimately, a design pressure was determined from the FEA and will be tested on the physical model.

2.1.3 Testing

The primary reason for testing is to gain an understanding of how the pressure vessel operates under design conditions while also ensuring the tank's integrity up to a certain factor of safety. The pressure vessel built in this study will be tested to ensure a factor of safety of 1.5, meaning that the pressure vessel should be able to maintain its shape and integrity at a pressure 50% higher than its design pressure. This will be accomplished by performing a hydrostatic pressure test. A hydrostatic test involves filling the pressure vessel with an incompressible liquid such as water and increasing the pressure until it meets that of a 1.5 safety factor. Since water is incompressible, the energy stored at higher pressures will be lower than that of a compressible gas. Therefore, if the tank were to burst, the water would simply seep or spray out instead of exploding as would happen with a gas. Additionally, strain gauges will be attached to parts of the vessel during the testing in order to gain acute changes in shape. This data will be compared with pressure, time, and stress to measure elongation and deformation.

2.1.4 Test Print

An image of a print using SLA is shown in Fig. 2.10 below to test the process of building this geometry as well as to evaluate what support structures might be needed.

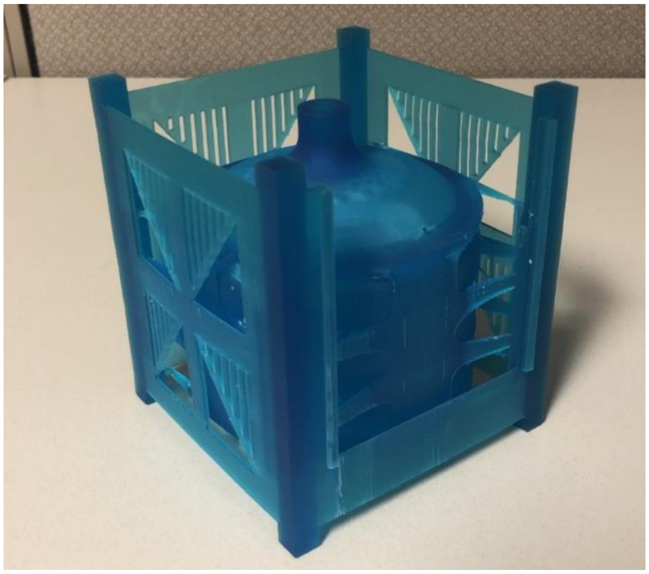

Figure 2.10 Test print of CubeSat propulsion module

2.2 Results

The results from these simulations led to a number of design improvements. The results and subsequent updates follow.

2.2.1 Results from FEA

An important component of any mechanical design process includes a thorough finite element analysis.

2.2.1.1 Pressure Vessel Stress Analysis

To begin the FEA procedure, the initial pressure vessel was tested. A material profile for Ti64 was put into Abaqus based on Renishaw's material data sheets [9]. A section was assigned with that material which was then assigned to the pressure vessel.

A pressure of 2200 psi was induced on the inside of the pressure vessel, and the hole of the vessel was fixed. A mesh of a 2 global value was assigned to the vessel. The part was meshed, and the job was submitted. Results from the pressure vessel stress analysis are shown below in Fig. 2.11.

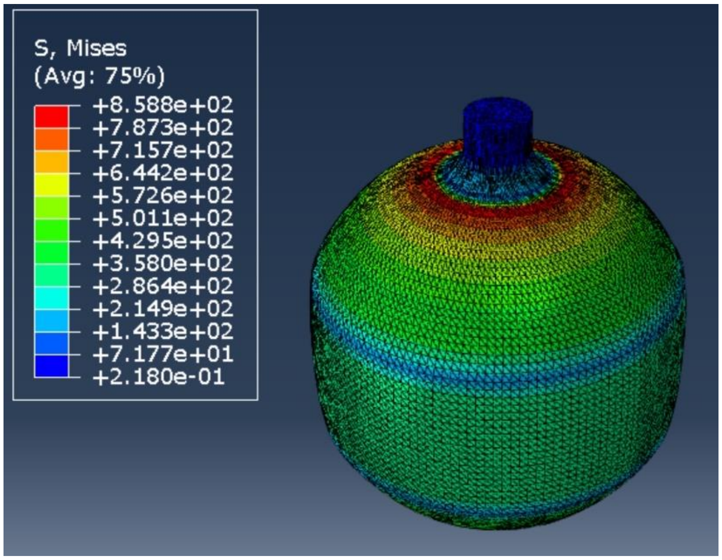

Figure 2.11 Results of FEA for pressure vessel

The maximum Von Mises stress found on the pressure vessel is 124,600 psi. The yield strength of Ti64 according to Renishaw is 142,900 psi. Therefore, under 2200 psi, the pressure vessel itself should be able to perform optimally. This gives it a safety factor of 2 since the intended operating pressure is 1100 psi.

However, there is a potential issue with the results found. Namely, the pressure vessel only seemed to be able to withstand around 2200 psi (15 MPa) of pressure though the initial thicknesses were designed for a very high safety factor and even scaled upward more to ensure integrity of printing. Why, then, is the FEA only suggesting that the vessel has a safety factor of 2? The issue does not stem from mesh convergence since the mesh was refined with similar values in maximum stress. The discrepancy in allowable pressure could stem from the fitting port, however. Figure 13 shows a zoomed-in view of the port.

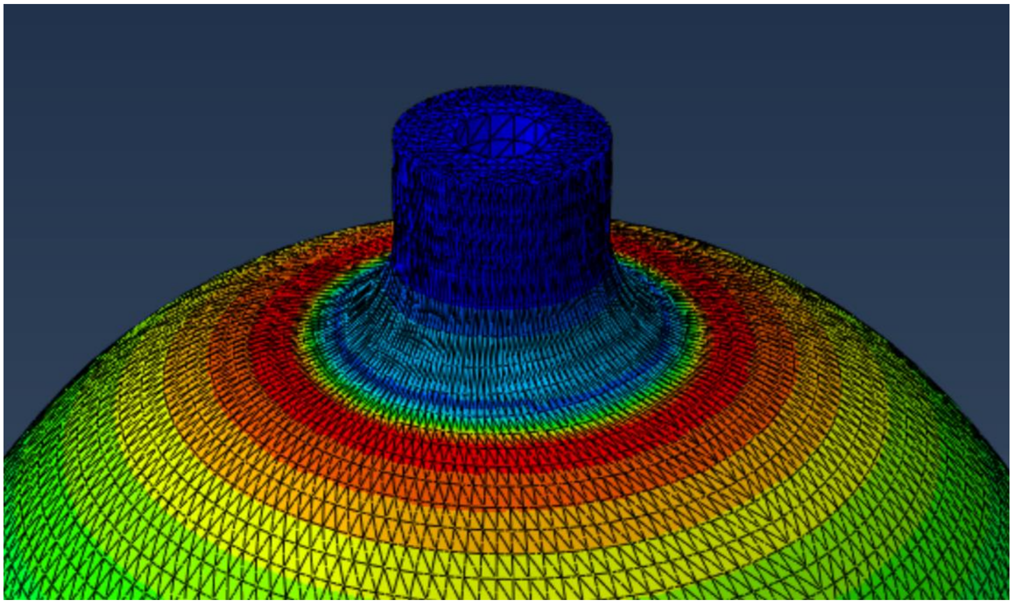

Figure 2.12 Zoomed-in view of port

It can be seen that much of the stress is concentrated in the region just outside of the port. This is expected because of the difference in thickness between the port portion's thickness and the thickness of the vessel directly adjacent to the port. Differences in thickness yield high stress gradients, which is not desirable in components, especially those under pressure. However, the port is an essential portion of the vessel because without it, propellant cannot be loaded into the system and a hydrostatic pressure test cannot be performed. One of the current activities in this study is to design a better port that can distribute stress more evenly across the region. High stress is often inevitable in high load environments; rather, it is the presence of a high stress gradient that is the issue. Also, improving the port to decrease stress gradient could in turn lower the overall stress concentration as a more efficient thickness profile could be designed.

2.2.1.2 Propulsion Module Stress Analysis

After analyzing the pressure vessel, the whole model was analyzed. Many of the parameters were the same as the analysis of the pressure vessel alone. A load of 2200 psi was induced in addition to the fixing of the port. A global mesh size value of 2 was assigned to the part, and a job was created and run. The mesh of the part is shown in Fig. 2.13 followed by the results of the FEA in Fig. 2.14.

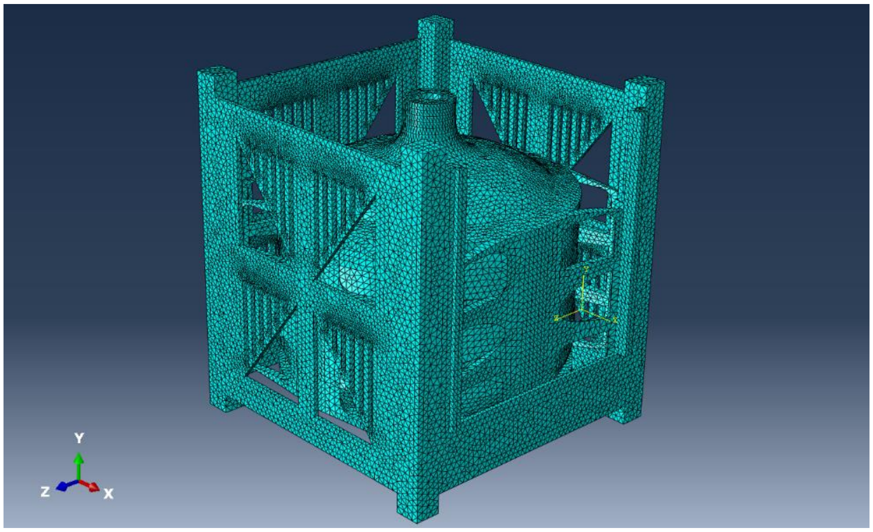

Figure 2.13 Mesh of CubeSat propulsion module

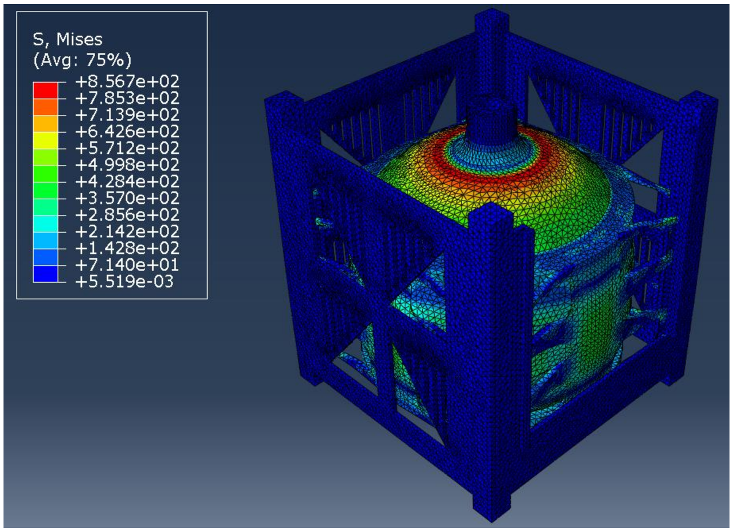

Figure 2.14 Stress analysis results of CubeSat propulsion module

The maximum stress found in the CubeSat module was 124,300 psi, which is very similar to the pressure vessel's maximum stress. This again gave the CubeSat propulsion module a safety factor of 2, which is above the 1.5 factor of safety required by the CubeSat Design Specification [1]. Once again, the highest stress was found at the base of the port. However, it can be seen that no other areas—most significantly the structural arms—were reaching very high stresses relatively. This suggests that the interface between the port and the vessel was the current limiting factor in the design.

2.3 Summary of Preliminary Findings

This study incorporates many aspects of engineering design. Because CubeSats have the advantage of being small, the turnaround for incorporating these design principles is relatively short. This has the stark advantage of allowing these systems to be worked on be small companies and universities within a reasonable time period and under a reasonable budget. The advantages of AM come into play as well as the ability to rapidly prototype these systems becomes apparent.

The actual design of this CubeSat propulsion module began with initial pressure calculations followed by 3D modeling of the pressure vessel. The vessel was integrated with the cube-like structure, and design on the structural arms began. Topology optimization was a very useful tool in designing the support arms of the CubeSat. This optimization was performed in Abaqus along with all of the stress analysis of the system. The stress analysis yielded reasonable results giving the CubeSat propulsion system a safety factor of 2. This can be improved through further optimization of some features of the CubeSat, namely the port for fittings. The interface between the port and the rest of the pressure vessel holds a large stress gradient, which can be mitigated somewhat through the resurfacing of that port of the vessel. Furthermore, one more issue can be remedied before printing. Although this study incorporates good AM practices, the topology optimization for the support arms did not yield AM-friendly results. These arms can be slightly modified to eliminate the need for extra support material during printing. Once these two issues are corrected, the module will be printed, heat-treated, and hydrostatically tested.

CHAPTER III

DESIGN REVISION, PRINTING, AND POST-PROCESSING

3.1 Design Revisions

In evaluating the efficacy of the original design and whether or not it would be effective for printing using metal additive manufacturing, the mockup model was observed throughout its build process. The most critical reason for these changes is that as errors are found in the plastic 3D-printed model, the issues stemming from these possibly small errors grow substantially as one transitions from plastic to metal printing. This is because of the general physics and principles of metal AM, namely the use of very tiny powder on the order of microns rather than the presence of a liquid resin. The heat associated with metal AM also demands robust structural supports that can effectively channel heat from the pressure vessel and support structure to the build plate during printing.

After making these design changes, further FEA was performed to ensure acceptable stress concentrations throughout the part before printing.

3.1.1 Model Changes

The two most significant changes to be made in the model were at the port of the pressure vessel and the structural arms attaching the pressure vessel to the cube. The primary issues were due to both stress concentration through the part or in local regions and also the friendliness of the design to metal AM, which was especially apparent in regard to the structural arms. The new features were modeled in SolidWorks and then exported to Abaqus for FEA to ensure that the changes were adequate to address the present issues.

3.1.1.1 Pressure Vessel Port

The primary issue with the port was both the stress concentration at the interface of the port and the pressure vessel as well as the general geometric dimension of the port itself.

The interface of the port and pressure vessel posed issues because of the thickness differential between the port stem and the actual pressure vessel. To address this issue material was added to the top of the vessel to better transition from the 2-mm thickness of the shell to the thicker portion of the port. This was in an effort to reduce stress concentration in region with large thickness gradient. In accordance to this, the lower head of the pressure vessel was scaled up to 2 mm as well to match the new thickness of the upper section.

The other motivation for editing of the pressure vessel was to best match the dimensions of the port needed for pressure testing, that being an 1/8-in tubing with an AN fitting. In order to find the optimal dimensions, discussions were held with machinists at NASA Marshall Space Flight Center (MSFC) in order to find the best method of shaping the port as to be optimal for post-machining processes. Here lies one of the focus points of modern design principles for AM. Though AM provides the distinct advantage of enabling complex models and geometry, the whole life of the additively manufactured part must be taken into account for design purposes. In this case, the part required a small port for a fitting to be machined into the part to allow for pressure testing. From a machinist’s point of view, hard angles and rectangular features are desirable for gripping during drilling. Because of this, a grip section was included in the model. In addition, sufficient space was given around the pilot hole as to allow for ample space for the port to be drilled. The size and location of the pilot hole was important too. A pilot hole that is too large can cause for undesirable vibration or shaking in the interface of the bit and the hole, ultimately damaging expensive bits used for these specific tasks. Additionally, an off-centered hole can be equally detrimental. Fortunately, in this case, lining up the hole was easily done as it is in the center of the part. The updated pressure vessel taking into account these changes is shown in Fig. 3.1 and Fig. 3.2.

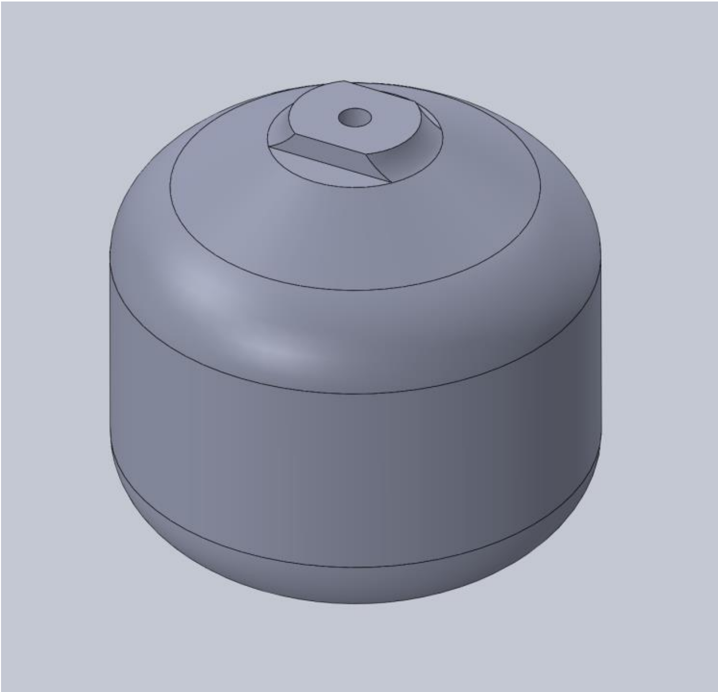

Figure 3.1 Updated pressure vessel

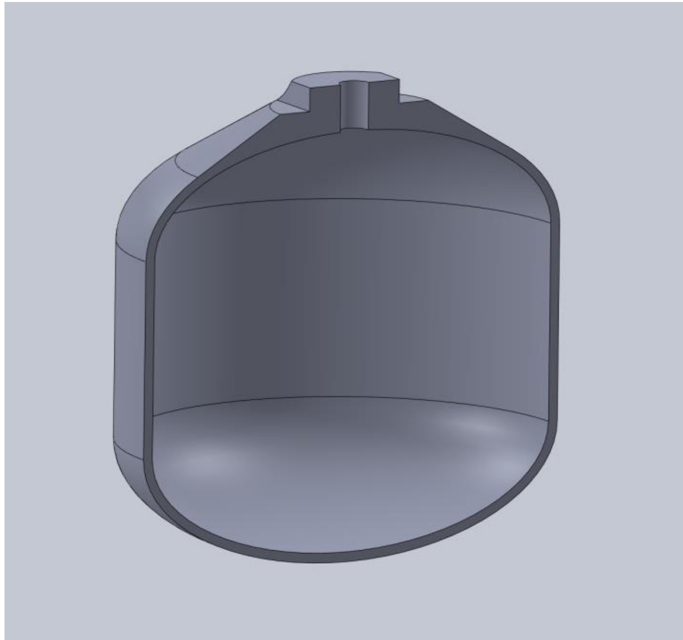

Figure 3.2 Cross-section view of updated pressure vessel

3.1.1.2 Structural Arms

Another issue in the plastic model of the CubeSat module was the design of the structural arms connecting the outer structural cube to the pressure vessel. The issue was evident during post-processing of the plastic model. Though the arms did undergo a simple topology optimization to find an efficient balance between structural integrity and volume, this structure was not optimized for additive manufacturing. This caused the need for structural supports to be printed on the part to keep it from failing. The problem arose when removing the part from the build plate and removing the structural supports. One of the stark advantages of a CubeSat is its size. However, this small size also makes it difficult to actually work within the small confines of the CubeSat, making the removal of these structural supports very difficult and strenuous. This difficulty in removing supports would only increase for similarly placed metal supports without compromising the integrity of several other components of the CubeSat.

The primary goal, then, in revising the design of the structural arms was to ensure that the arms could be printed without the presence of support structure. This would eliminate the potential of impossible-to-remove structures, ultimately ensuring that mass of the part is decreased. This was achieved by eliminating the bridged section appearing in the original arm and opting for simple branch structures connecting the cube to the vessel though still in the same general pattern laid out from the topology optimization. A finished model of the structural arm is shown in Fig. 3.3.

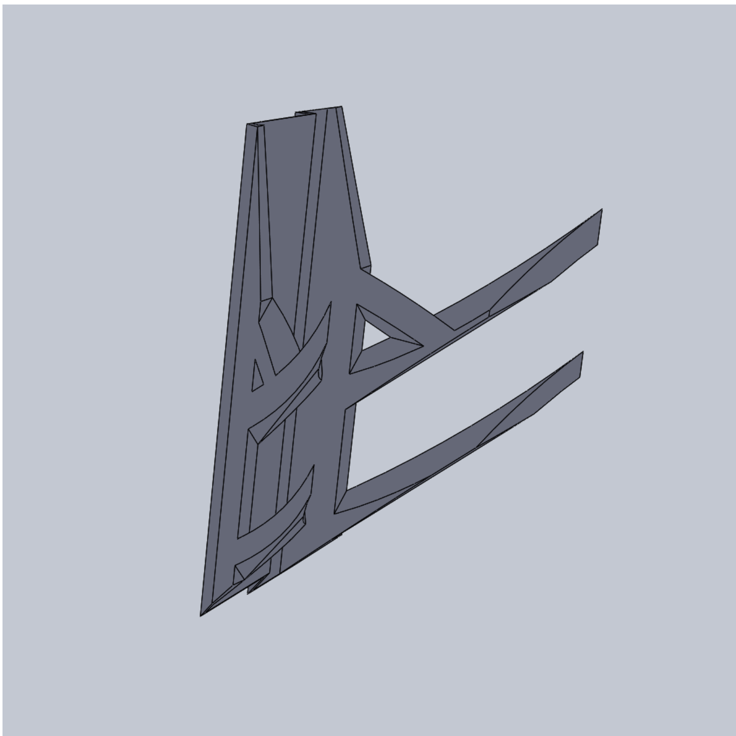

Figure 3.3 Updated structural arm

Further optimization could be performed by pursuing a more sophisticated topology optimization that takes into account the need for printability.

3.1.2 Updated Finite Element Analysis

The updated FEA was in much part similar to the first FEA procedure outlined in Chapter II. However, the general procedure will be overviewed with respect to the new model. The completed assembly incorporating the updated parts is shown in Fig. 3.4.

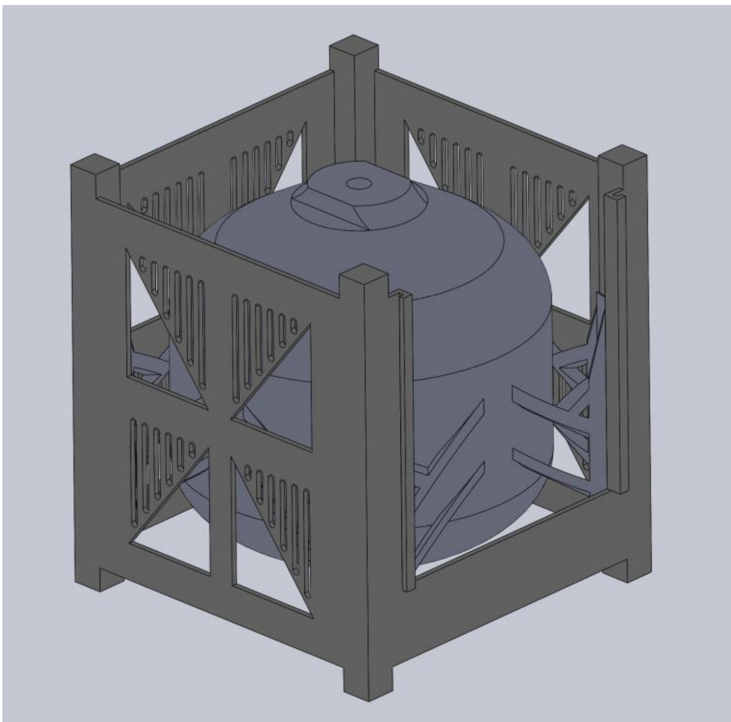

Figure 3.4 View of full CubeSat assembly

The loading and boundary conditions were almost identical to the previous method with a restrained inner surface of the port and an induced pressure load of 3200 psi (22 MPa) to the inner surface of the vessel. A diagram depicting these loading and boundary conditions is shown in Fig. 3.5.

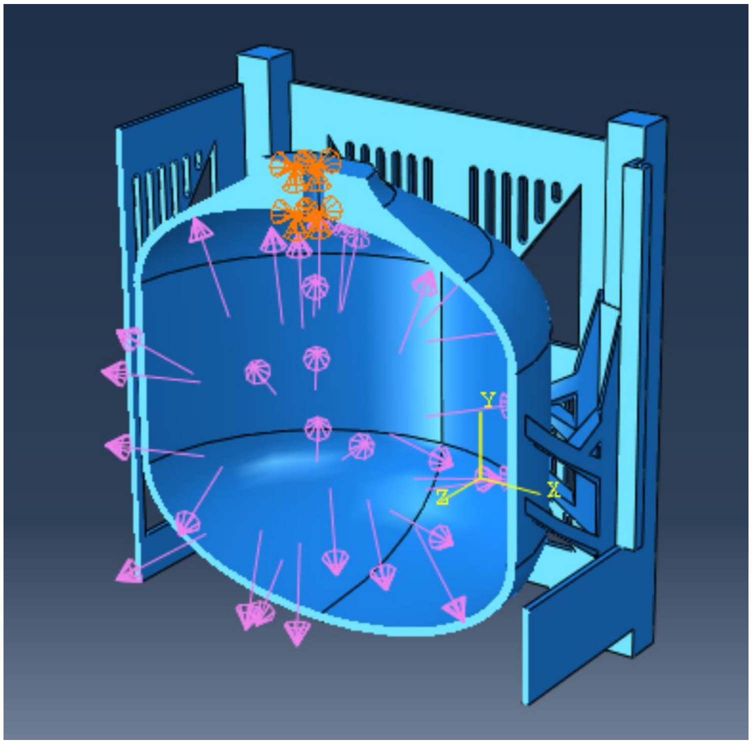

Figure 3.5 Loading and Boundary Conditions on updated model

Once again, quadratic tetrahedral elements were used with a global value size of 2.6. This completed mesh is shown in Fig. 3.6.

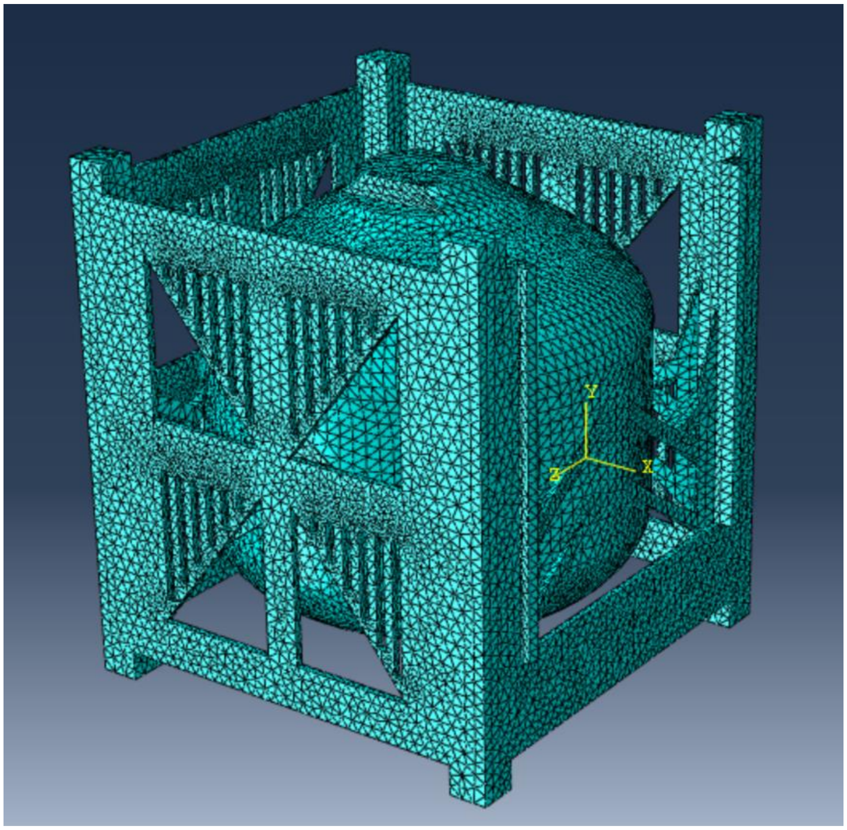

Figure 3.6 Mesh of CubeSat assembly

The results of the job are shown in Fig. 3.7 and Fig. 3.8. These include both a full view of the part in addition to a section view of the part.

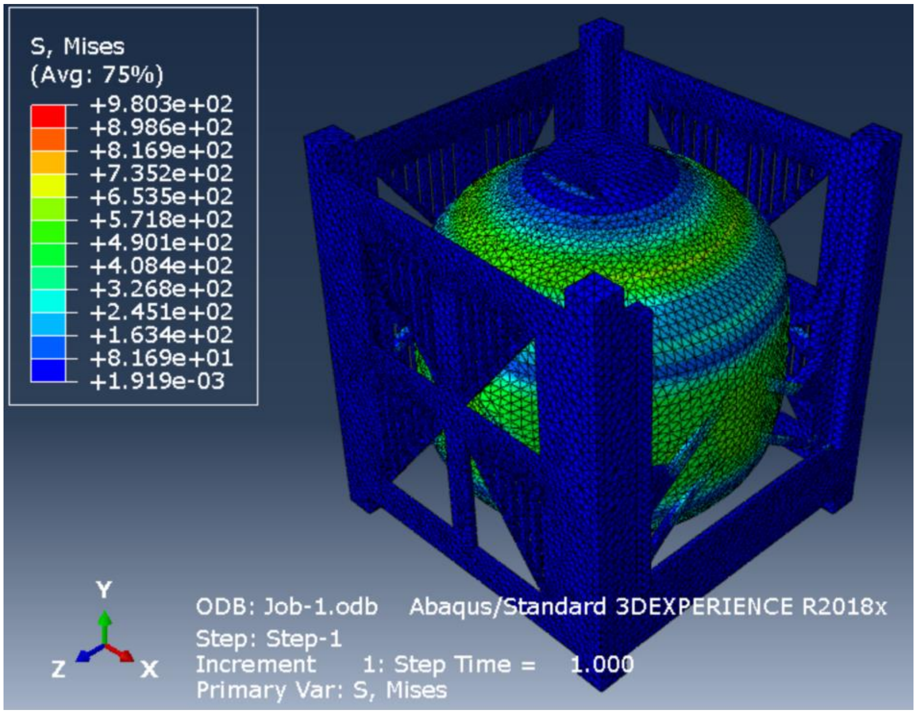

Figure 3.7 Full view of stress analysis visualization

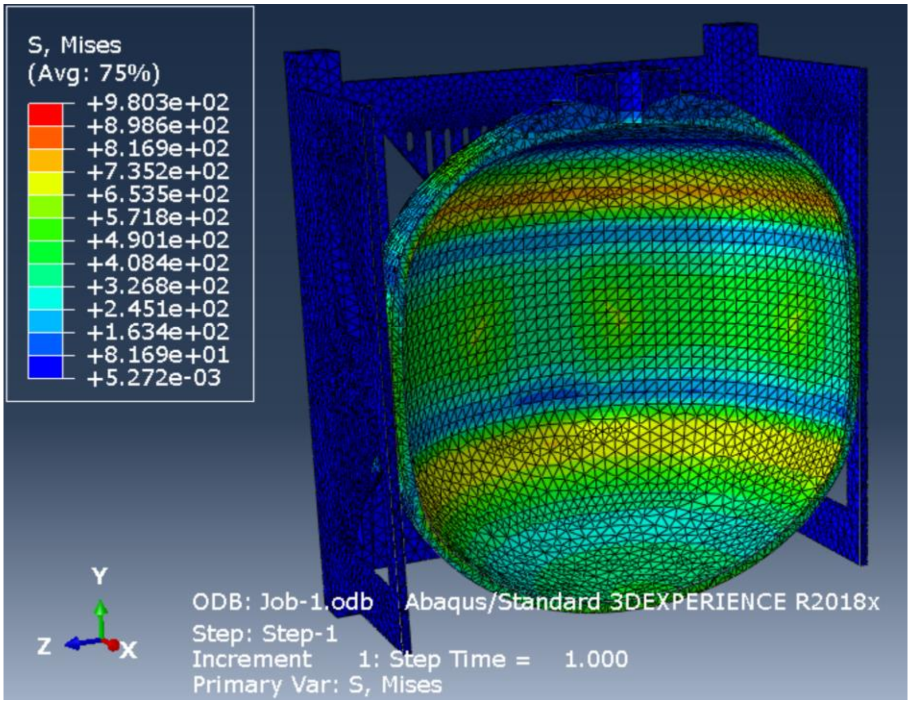

Figure 3.8 Cross-section view of stress analysis visualization

It should be noted that no visible highest stress are apparently in view of the part in both the full view and the section view of the results of the FEA. That is an indicator that an outlier internal stress may be located in the part. As it stands, the maximum Von Mises stress within the part is 980.3 MPa, which is below the specified yield stress given by Renishaw [9]. However, the internal stresses are observed to find the stress anomaly in the part. The first view of this cut out is shown in Fig. 3.9.

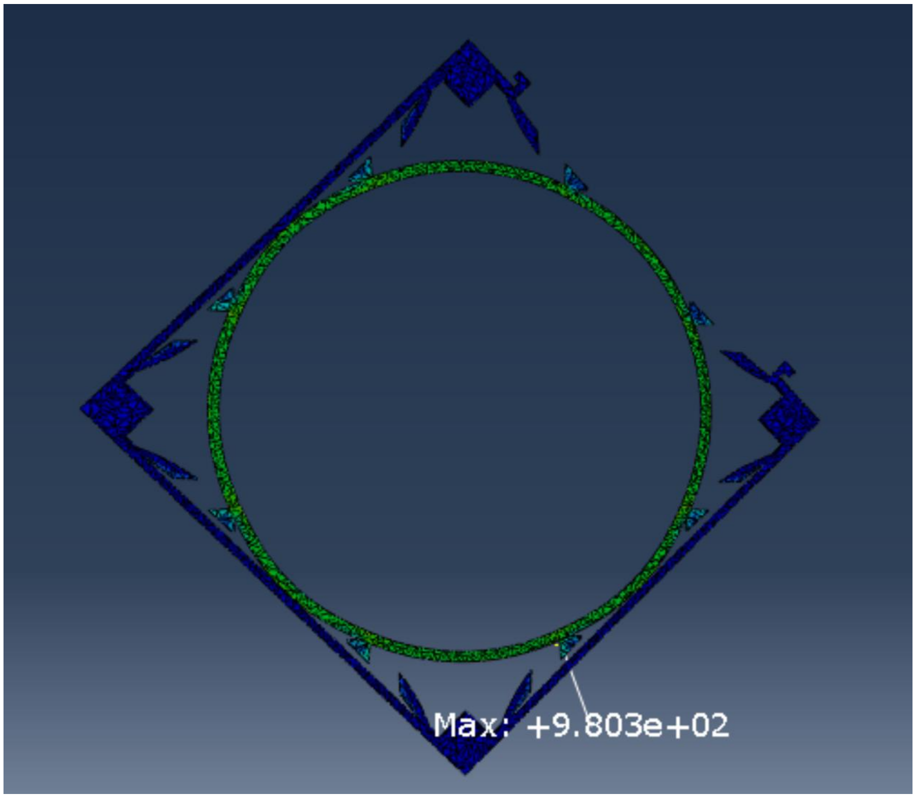

Figure 3.9 Vertical cross-section view including maximum stress point

From this view, it is apparent that the maximum stress was found at the intersection of a structural arm and the pressure vessel. However, it does not appear that other areas of the model exhibit a stress of this magnitude. Another view is established that could more accurately indicated the maximum stress in the part, which is shown in Fig. 3.10.

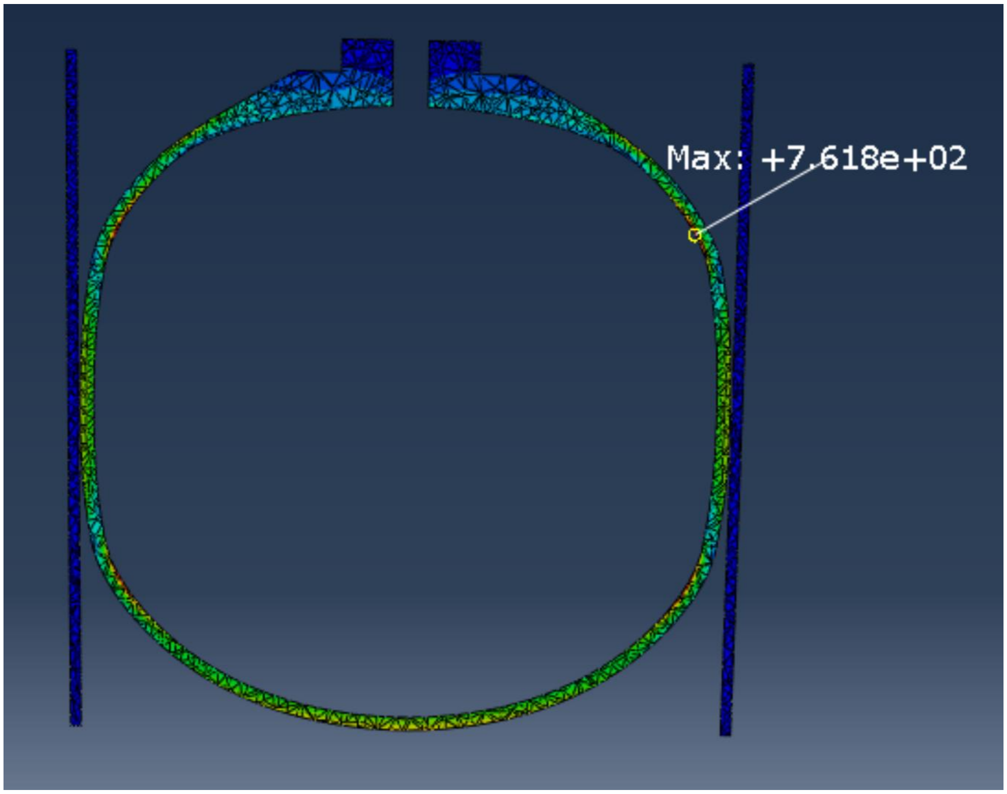

Figure 3.10 Horizontal cross-section view

In every other sliver of the CubeSat, both in the vertical and horizontal orientations, the maximum stress was found to be 761.8 MPa. Given that the specified yield stress of the material is 985 MPa, it appears that the part did not reach that yield stress, indicating that this particular test is successful. In fact, with the prescribed pressure load of 22 MPa, the part exhibits a safety factor of over 3.5.

3.2 Printing and Post-Processing

After successful FEA, the part was exported as an .STL file and pre-processed for 3D-printing, mostly consisting of adding structural supports to the part, notably around the edges, at the bottom of the pressure vessel, and inside the pressure vessel. Out of these regions, the support structures can all be removed except for those inside of the pressure vessel. However, the internal structural supports' volume is negligible compared to the useful volume inside the vessel for propellant.

3.2.1 First Build

The first attempted build ended after a few hours. This was due to inadequate thickness of structural supports which allowed residual stress to build up in the part and caused deformation in the part. Two examples of this are shown. The first one of these is shown in Fig. 3.11.

Figure 3.11 Example of bowing defect in the CubeSat

This figure shows bowing in the part due to the residual stress buildup described previously. Thicker structural support can prevent this. A second example is shown in Fig. 3.12.

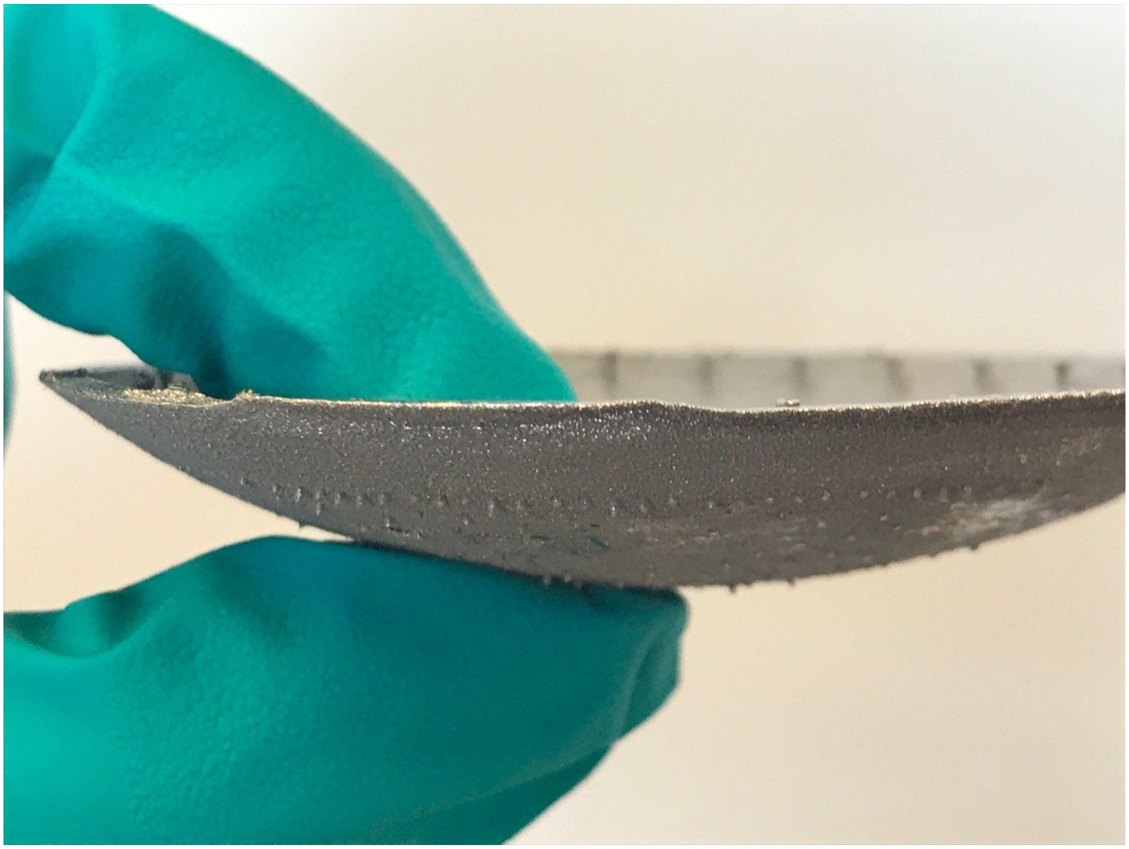

Figure 3.12 Example of knife edge defect in the pressure vessel section

This figure shows a phenomenon called a “knife edge” in which the residual stresses cause the edge of the build to curl up. As subsequent layers are deposited, this curling worsens, resulting in a sharp edge.

3.2.2 Finished Build

Several views of the final build are shown in Fig. 3.13, Fig. 3.14, and Fig. 3.15. Note that two full-sized models and two scaled down models of the part are built.

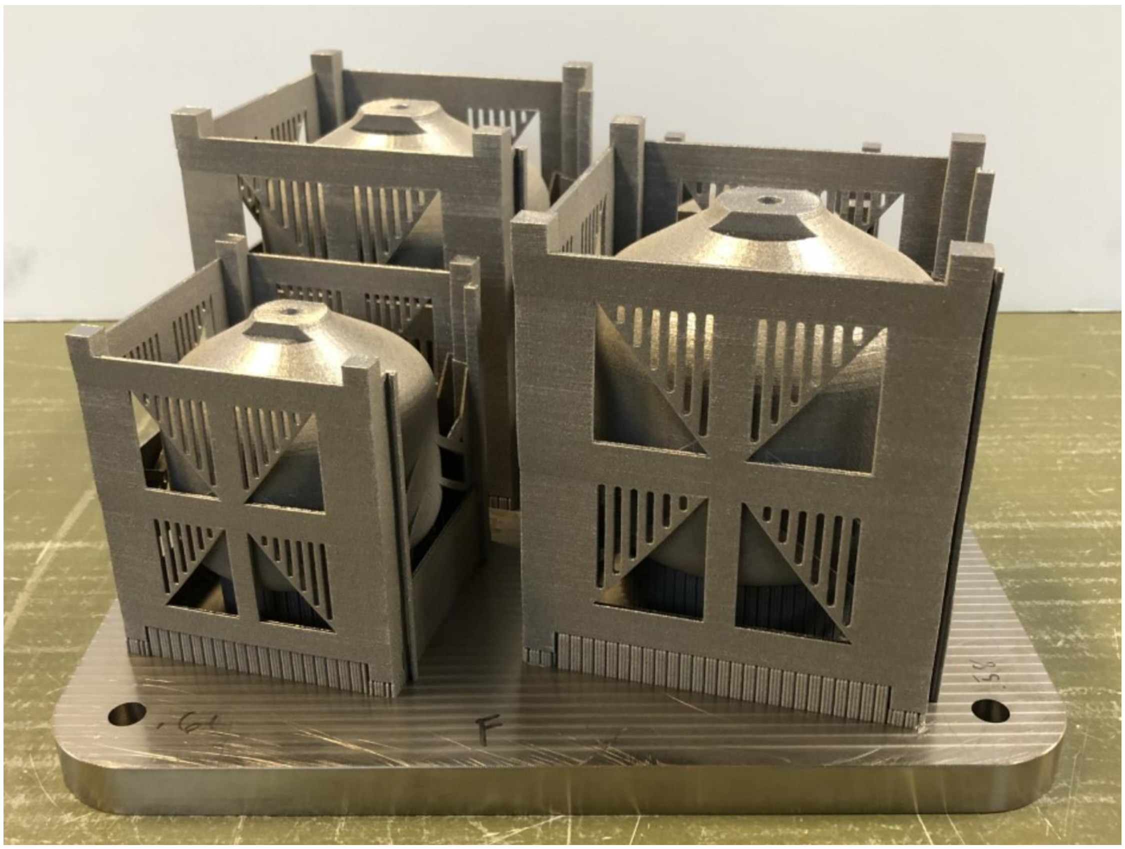

Figure 3.13 Frontal view of completed CubeSat build

Figure 3.14 Top view of completed CubeSat build

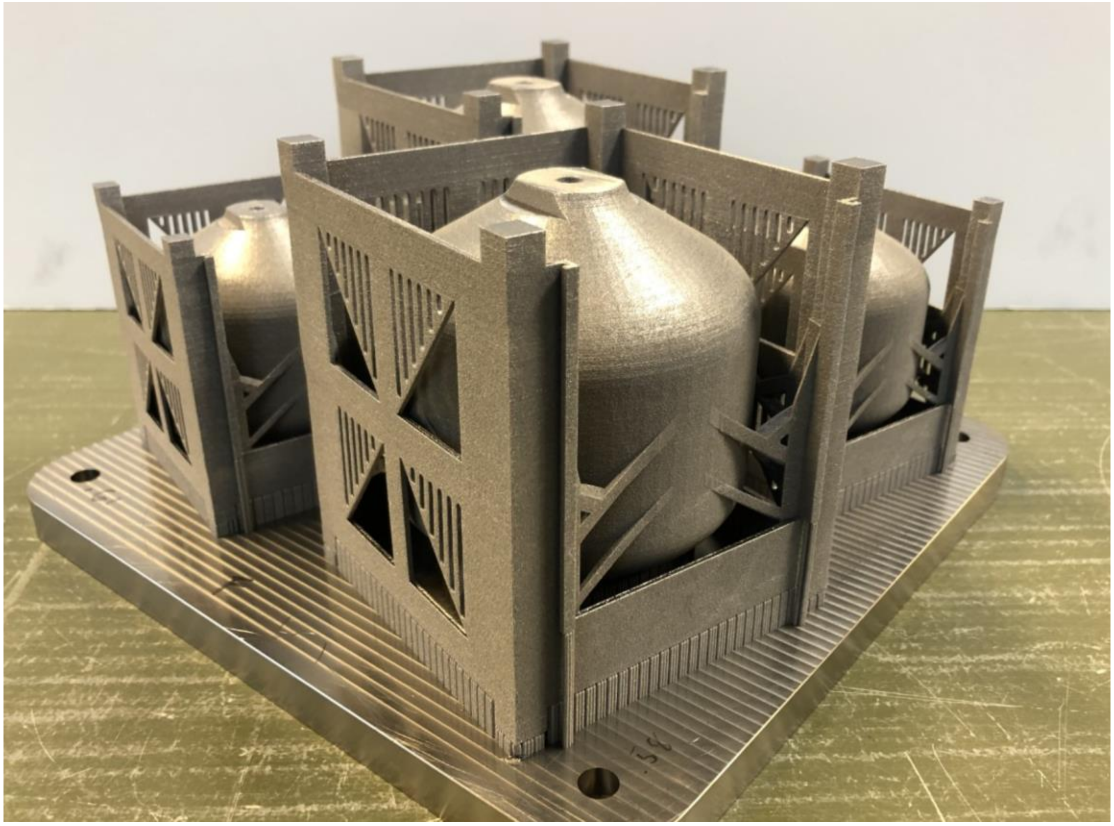

Figure 3.15   Frontal diagonal view of completed CubeSat build

Overall the build came out very well. There are no significant defects in the printed parts, but there are a couple of minor defects such as some peel in Fig. 3.16 and slight abrasion in Fig. 3.17.

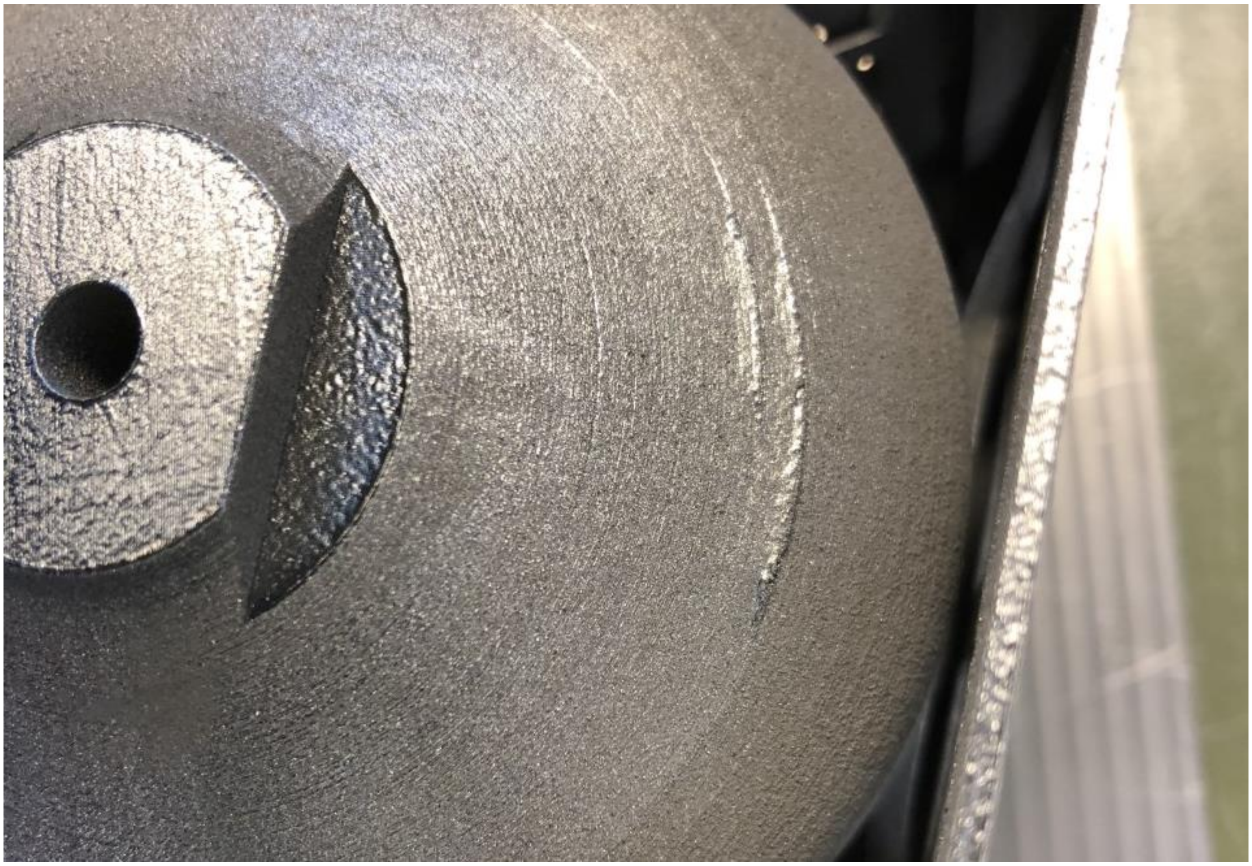

Figure 3.16 Minor absence of adhesion on upper pressure vessel

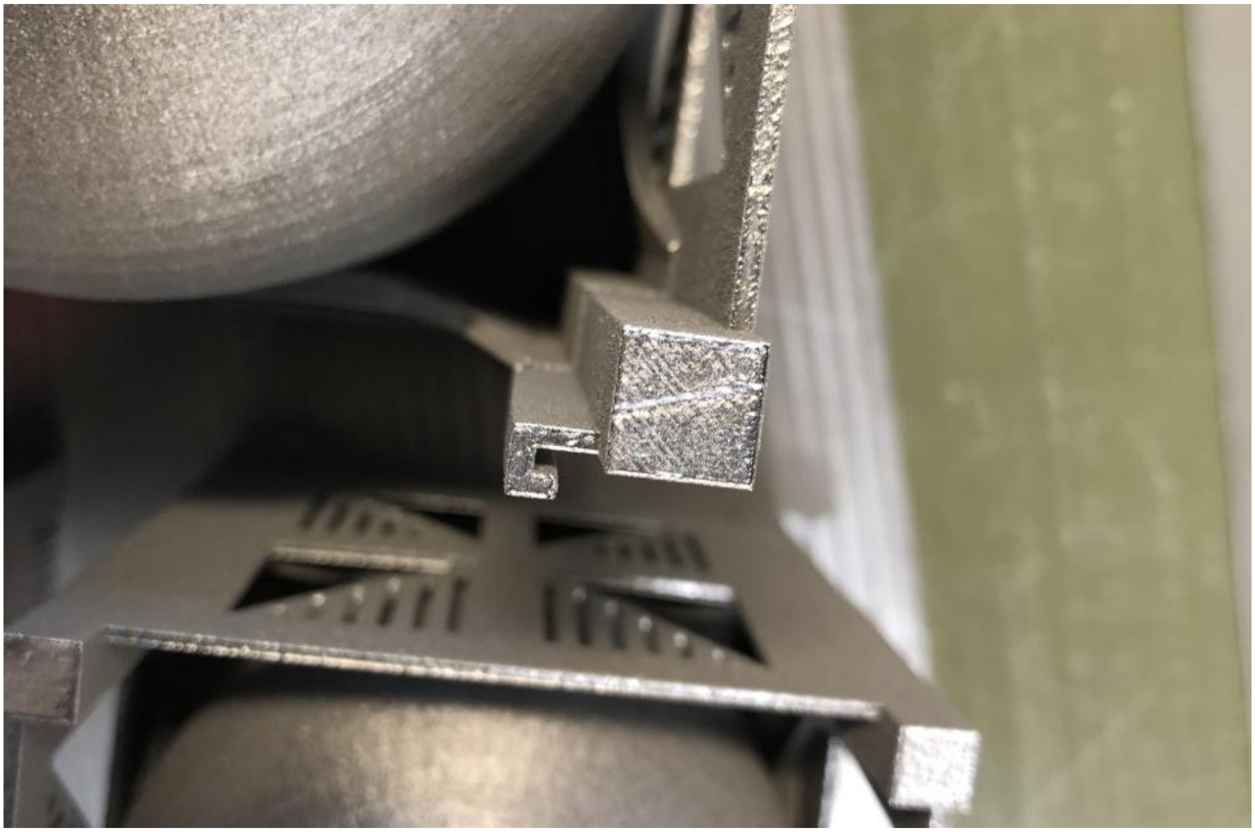

Figure 3.17 Slight abrasion on CubeSat

3.2.3 Further Post-Processing

After printing, the finished modules along with the substrate underwent heat treatment to alleviate any remaining residual stresses in the part. This required that argon gas flow through the heat chamber during the treatment. It was later discovered that oxidation did occur on the part during the heat treatment for unknown reasons. This could be because of an insufficient amount of argon flowing through the chamber during heat treatment. The parts are being removed, and they will be examined further to evaluate how deep the oxidation layer is and whether or not it is detrimental to the behavior and integrity of the module.

CHAPTER IV

FUTURE WORK AND CLOSING REMARKS

4.1 Future Work

There is much potential for future work for this study. Most notably, the testing campaign has yet to be fleshed out for the pressure vessel. The primary barrier holding this back is the need to find whether or not the oxidation present on the module from heat treatment is detrimental to the structural integrity of the part. If it is deemed detrimental, any findings from a pressure test will most likely not be very significant in the effort to verify the validity of the design and simulation activities.

The simulation activities could also be updated to include more sophisticated techniques such as a full topology optimization for the support arms. In addition, different meshing strategies could be implemented to reduce computational time including modeling the pressure vessel as a conglomerate of shell elements.

Further iterations of the design could also include modifications to the geometry of the CubeSat in an effort to make better use of the CubeSat volume as well as how it interfaces with other components of a CubeSat such as the avionics and actual thruster.

4.2 Conclusion

This study has accomplished many of its goals of predicting whether or not additive manufacturing is a viable method of fabrication for small satellites including CubeSats. Much work went into the initial process to come up with mission requirements including propellant and pressure calculations which can be valuable for future studies. Additionally, the simulation efforts also present valuable, practical ways to verify design strategies as shown in the study. The last step that will be useful to future studies is to continue with the testing strategy specified previously, which will provide verification of viability for many of the methods and ideas described.

REFERENCES

[1] The CubeSat Program, Cal Poly SLO, "CubeSat Design Specification," Rev. 13, 2014.

[2] Air Force Space Command, "Range Safety User Requirements Manual Volume 3 Launch Vehicles, Payloads, and Ground Support Systems Requirements," *AFSPMAN 91-710*, Vol. 3, 2004, (Rev. 2015).

[3] Anis, A., "Cold Gas Propulsion System - An Ideal Choice for Remote Sensing Small Satellites," Remote Sensing, Boris Escalante-Ramirez, IntechOpen, 13 June 2012, pp. 447-462

doi: 10.5772/37149.

[4] Tummala, A. R., and Dutta, A., "An Overview of Cube-Satellite Propulsion Technologies and Trends," *MDPI Aerospace*, Vol. 4, No. 58, 9 December 2017.

[5] Askeland, D. R., Phule, P. P., *The Science and Engineering of Materials*, Ch.14, 2006.

[6] Martinez, M. G., "PFC: AlSi10Mg Parts Produced by Selective Laser Melting (SLM)," *Ku Leuven Universidad Carlos III de Madrid*, 31 May 2013.

[7] Gorsse, S., et al., "Additive manufacturing of metals: a brief review of the characteristic microstructures and properties of steels, Ti-6Al-4V and high-entropy alloys," *Science and Technoogy of Advanced Materials*, Vol. 18, No. 1, 2017, pp. 584-610

doi: 10.1080/14686996.2017.1361305

[8] Rafi, H. K., et al., "A comparison of the tensile, fatigue, and fracture behavior of Ti-6Al-4V and 15-5 PH stainless steel parts made by selective laser melting," *The International Journal of Advanced Manufacturing Technology*, Vol. 69, No. 5-8, 2013, pp.1299-1309.

[9] Renishaw, "Ti6Al4V ELI-0406 powder for additive manufacturing," *Renishaw*.

[10] Renishaw, "AlSi10Mg-0403 powder for additive manufacturing," *Renishaw*.

[11] Gradl, P. R., et al., "Development and Hot-fire Testing of Additively Manufactured Copper Combustion Chambers for Liquid Rocket Engine Applications," *AIAA/SAE/ASEE Joint Propulsion Conference*, Atlanta, Georgia, 2017.

[12] Hopkins, R. C., "Additive Manufacturing: An Enabling Technology for the MoonBEAM 6U CubeSat Mission," *NASA/TM*, 2017.

[13] Romei, F., Grubisic, A. N., Gibbon, D., "Manufacturing of a High-Temperature Resistojet Heat Exchanger by Selective Laser Melting," *Acta Astronautica*, No. 138, 2017, pp. 356-368.

[14] Tam, W., Wlodarczyk, K., Kawahara, G., "Additive Manufactured Pressure Vessel Shell," *Space Propulsion 2018*, Seville, Spain, 14-18 May 2018.

[15] Carpenter, C., et al., "Test Results for the MPS-120 and MPS-130 CubeSat Propulsion Systems," *Aerojet Rocketdyne*, URL: http://mstl.atl.calpoly.edu/~bklofas/Presentations/SummerWorkshop2014/SSC14-WK-36_Carpenter.pdf

[16] Solorzano, G. A., "Development and Prototype Validation of an Additive Manufactured CubeSat Propulsion Tank," M.S. Thesis, Mechanical Engineering Dept., Embry-Riddle Aeronautical Univ., 2015.

[17] Nahmany, M., et al., "Structural Properties of EB-Welded AlSi10Mg Thin-Walled Pressure Vessels Produced by AM-SLM Technology," *Journal of Materials Engineering and Performance*, Vol. 26, No. 10, 2017, pp. 4813-4821.

doi: 10.1007/s11665-017-2953-7

[18] Gaudenzi, P., "Revisiting the configuration of small satellites structures in the framework of 3D Additive Manufacturing," *Acta Astronautica*, Vol. 146, 2018, pp. 249-258.

[19] Diegel, O., et al., "Tools for Sustainable Product Design: Additive Manufacturing," *Journal of Sustainable Development*, Vol. 3, No. 3, 2010, pp. 68-75.

[20] Renishaw, "Design for Metal AM – A Beginner's Guide," *Renishaw*, URL: https://www.renishaw.com/en/design-for-metal-am-a-beginners-guide--42652 [retrieved 17 August 2017].

[21] Renishaw, "Is Topological Optimization Really Optimal," *Renishaw*, URL: https://www.renishaw.com/en/is-topological-optimisation-really-optimal--42112 [retrieved 17 August 2017].

[22] ASME, "ASME Boiler & Pressure Vessel Section VIII, Division I," 1995.

[23] Jones, J. W., "Finite Element Analysis of Pressure Vessels," *Bulletin*, 1989.

[24] SolidWorks, "Understanding Nonlinear Analysis," *Real Insight*